**Dietmar Rieder**

# Prediction and identification of large scale chromatin decondensations

Master Thesis

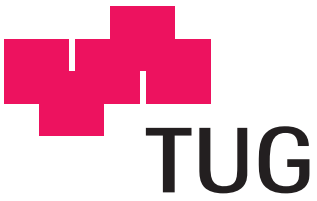



Institute for Biomedical Engineering, Graz University Of Technology, Graz Austria[1]

National Institutes Of Health, Bethesda, Maryland USA[2]

Institute for Molecular Biology, Biochemistry and Microbiology, Graz Austria[3]

| | |
|---|---|
| Supervisor: | Ao.Univ.-Prof. Dipl.-Ing. Dr.techn. Zlatko Trajanoski[1] |
| | Dr. James McNally[2] |
| Evaluator: | Ao.Univ.-Prof. Dr. Günther Koraimann[3] |

Graz, May 2003

**For Lisi**

# Abstract

The objectives of this work were the prediction and the identification of large-scale chromatin decondensations within interphase chromosomes in a natural system. The total length of chromosomal DNA in eukaryotic cells is up to a hundred thousand times the cell's length, therefore the DNA is packed into a higher-order structure to fit into the limited volume of the nucleus. Upon transcription, the densely packed chromatin has to decondense in active regions in order to allow an interaction of DNA binding molecules with the DNA. In order to predict such decondensations, gene expression data - derived from DNA microarray - was mapped to chromosomal positions and a scoring system was developed which made it possible to find regions with different transcriptional activity. The scoring sytsem revealed a region on human chromosome 22, which shows different levels of gene expression in three cell lines (K-562, Jurkat and Raji). This result led to the prediction, that a large-scale chromatin decondensation can be identified in the more active cell lines, and that the compaction rate will decrease with an increased transcriptional activity. To identify large-scale chromatin decondensations, the region was studied by means of DNA flourescence in situ hybridization (FISH). Two probes (BACs) were hybridized to the begin and the end of the region, and the distance between the resulting fluorescence signals was measured in the three cell lines. The measurements of the distance in multiple cells from each cell line, revealed that the predicted large-scale chromatin decondensations exist and that the structure within the decondensed region is consistent with the "chromonema fiber" model of higher-order chromatin organisation. For a verifaction the cells were treated with DRB (5,6-dichloro-1-$\beta$-D-ribofuranosylbenzimidazole), in order to inhibit transcription. In treated cells the open region recondensed, which shows that the large-scale decondensation was due to transcriptional activity.

In conclusion the results show that it is possible to predict and identify large-scale chromatin decondensations caused by gene transcription.

**Keywords:** chromatin decondensation, chromonema fiber, interphase, FISH, transcription

# Kurzfassung

Ziel dieser Arbeit war es, "umfangreiche Chromatin Dekondensationen" vorherzusagen und diese dann zu identifizieren. Die Gesamtlänge der chromosomalen DNA in eukaryotischen Zellen beträgt ein hunderttausendfaches der Länge einer Zelle. Um Platz im begrenzten Volumen eines Zellkerns zu finden, ist die DNA als Struktur höherer Ordnung verpackt. Während der Gentranskription in der Interphase muss das dicht gepackte Chromatin in aktiven Bereichen eine dekondensierte Konformation annehmen, damit eine Interaktion von DNA-bindenden Molekülen mit der DNA möglich wird. Um solche Dekondensationen vorhersagen zu können, wurden Genexpressionsdaten von DNA-Microarrays auf die chromosomale Position eines jeweiligen Gens abgebildet und ein Bewertungssystem entwickelt, das es ermöglichte Bereiche mit unterschiedlicher Genexpression ausfindig zu machen. Mit Hilfe des Bewertungssystems wurde ein Bereich am menschlichen Chromosom 22 gefunden, der in drei Zelllinien (K-562, Jurkat und Raji) eine unterschiedliche transkriptionelle Ativität aufweist. Die Annahme war, dass man in den aktiveren Zelllinien umfangreiche Chromatin Dekondensationen, in diesem Bereich beobachten könne, und dass die Packungsdichte bei einer erhöhten Genexpression abnimmt. Um solche umfangreiche Chromatin Dekondensationen identifizieren zu können, wurde der Bereich mit Hilfe der DNA FISH Technik untersucht. Zwei Sonden (BACs) wurden an den Anfang und das Ende des Bereichs hybridisiert, worauf dann in den drei Zelllinen der Abstand zwischen den beiden resultierenden Fluoreszenzsignalen gemessen wurde. Die Messungen des Abstandes in mehreren Zellen jeder Zelllinie ergaben, dass die vorhergesagten Dekondensationen tatsächlich existieren, und dass die Struktur des dekondensierten Bereichs dem "Chromonema Fiber Model" für die Chromatin Organisation höherer Ordnung entspricht. Als Kontrolle wurden die Zellen mit DRB (5,6-Dichloro-1-$\beta$-D-Ribofuranosylbenzimidazol) behandelt, um die Transkription zu inhibieren. Der Bereich lag nach der Inhibition wieder dicht gepackt vor, was beweist, dass die Dekondensation durch transkriptionelle Aktivität hervorgerufen wurde. Es ist also möglich, Chromatin Dekondensationen vorherzusagen und zu identifizieren.

**Schlüsselwörter:** Chromatin Dekondensation, Chromonema Fiber, Interphase, FISH, Transkription

# Contents

# List of Figures

# Glossary

**acrocentric** a chromosome with the centromere towards one end is acrocentric.

**awk** is a pattern scanning and processing language. It scans each input file for lines that match any of a set of specified patterns.

**API** stands for "Application Programming Interface" and provides a set of functions and classes that can be used to develop an application.

**BAC** bacterial artificial chromosomes are vectors similar to standard E. coli plasmid vectors except that they contain the origin and genes encoding the ORI-binding proteins required for plasmid replication from a naturally occurring large E. coli plasmid called the F-factor. Inserts can be up to 300 Kbp in size.

**C** is a programming language.

**CCD** a charge coupled device is a collection of tiny light-sensitive diodes, which convert photons (light) into electrons (electrical charge). A CCD camera can be used to acquire digital images.

**cDNA** complementary DNA is a form of DNA prepared in the laboratory using messenger RNA (mRNA) as template, i.e. the reverse of the usual process of transcription in cells; the synthesis is catalyzed by reverse transcriptase. cDNA thus has a base sequence

that is complementary to that of the mRNA template; unlike genomic DNA, it contains no noncoding sequences (introns).

**centromere** constricted portion of a mitotic chromosome where sister chromatids are attached. It is required for proper chromosome segregation during mitosis and meiosis.

**chromatid** one copy of a duplicated chromosome, formed during the S phase of the cell cycle, that is still joined at the centromere to the other copy; also called sister chromatid. During mitosis, the two chromatids separate, each becoming a chromosome of one of the two daughter cells.

**chromatin** complex of DNA, histones, and nonhistone proteins from which eukaryotic chromosomes are formed. Condensation of chromatin during mitosis yields the visible metaphase chromosomes.

**CPAN** stands for Comprehensive Perl Archive Network; it's a globally replicated trove of Perl materials.

**cy3** fluorescent dye, green; used for labeling RNA in microarray experiments.

**cy5** fluorescent dye, red; used for labeling RNA in microarray experiments.

**deconvolution** is a process of relocating signal scatter and out-of-focus information present in digital images. The image seen in the microscope also contains blur from out-of-focus light and light scatter in the specimen. This blur results from the convolution of the specimen with the microscope's Point Spread Function (PSF). By reversing this blurring through the constrained-iterative deconvolution process, the image is clarified and its data is quantitatively restored.

**DNA** deoxyribonucleic acid is a long linear polymer, composed of four kinds of deoxyribose nucleotides, that is the carrier of genetic information.

**DNase** an enzyme that catalyzes the cleavage of DNA. DNAase I is a digestive enzyme, that degrades DNA into shorter nucleotide fragments.

**euchromatin** less condensed portions of chromatin, including most transcribed regions, present in interphase chromosomes. See also heterochromatin.

**exon** segments of a eukaryotic gene (or of its primary transcript) that reaches the cytoplasm as part of a mature mRNA, rRNA, or tRNA molecule. See also intron.

**grep** program that searches the named input files (or standard input if no files are named) for lines containing a match to the given pattern.

**heterochromatin** regions of chromatin that remain highly condensed and transcriptionally inactive during interphase.

**insert** piece of DNA that is cloned into a vector.

**intron** part of a primary transcript (or the DNA encoding it) that is removed by splicing during RNA processing and is not included in the mature, functional mRNA, rRNA, or tRNA;

**JPEG** compressed graphics format.

**metaphase** mitotic stage at which chromosomes are fully condensed and attached to the mitotic spindle at its equator but have not yet started to segregate toward the opposite spindle poles.

**mitosis** in eukaryotic cells, the process whereby the nucleus is divided to produce two genetically equivalent daughter nuclei with the diploid number of chromosomes.

**NCBI** National Center for Biotechnology Information. NCBI creates public databases, conducts research in computational biology, develops software tools for analyzing genome data, and disseminates biomedical information.

**ONC** Over Night Culture. Cell grown over night.

**oncogene** a gene whose product is involved either in transforming cells in culture or in inducing cancer in animals. Most oncogenes are mutant forms of normal genes (proto-oncogenes) involved in the control of cell growth or division.

**PBS** Phosphate-Buffered Saline; 0.02 M sodium phosphate buffer with 0.15 M sodium chloride

**plasmid** small, circular extrachromosomal DNA molecule capable of autonomous replication in a cell. Commonly used as a cloning vector.

**PNG** Portable Network Graphics. Graphics format.

**RNA** ribonucleic acid is a linear, single-stranded polymer, composed of ribose nucleotides, that is synthesized by transcription of DNA or by copying of RNA. The three types of cellular RNA - mRNA, rRNA, and tRNA - play different roles in protein synthesis.

**sed** is a stream editor. A stream editor is used to perform basic text transformations on an input stream.

**sh** is a command programming language that executes commands read from a terminal or a file.

**sort** is a program which sorts lines of all the named files together and writes the result on the standard output.

**SSC** Saline-Sodium Citrate buffer for ISH procedures.

**STS** stands for "sequence tagged sites"; short sequences that are operationally unique in the genome, used to generate mapping reagents.

**vector** in cell biology, an agent that can carry DNA into a cell or organism.

**XML** Extensible Markup Language (XML) is a simple, very flexible text format. Originally designed to meet the challenges of large-scale electronic publishing, XML is also playing an increasingly important role in the exchange of a wide variety of data on the Web and elsewhere.

**zip archive** zip files are "archives" used for distributing and storing files. Zip files contain one or more files. Usually the files "archived" in a Zip are compressed to save space. Zip files make it easy to group files and make transporting and copying these files faster.

# Chapter 1

# Introduction

## 1.1 DNA and its organization

The genetic information of living organisms is carried by DNA, which can be seen as a storehouse, or cellular library, that contains all the information required for building cells and tissues. DNA is an enormously long polymeric molecule. Basically it consits of a sequence of four different subunits, the so called nucleotides. Cellular DNA molecules can be as long as several hundred million nucleotides, arranged in an irregular but non-random sequence. Every million nucleotides take up a linear distance of 3.4 x $10^5$ nm (0.034 cm). The human genome consists of about 6 x $10^9$ nucleotide pairs, organized in 2 x 23 different DNA molecules, the chromosomes - each containing 50 x $10^6$ to 250 x $10^6$ nucleotide pairs. DNA molecules of this size have a linear length of 1.7 to 8.5 cm.

### 1.1.1 Basic DNA packing

Because the total length of chromosomal DNA in cells is up to a hundred thousand times the cell's length, the packing of DNA into a compact structure is crucial. The DNA must fit in a nucleus of only a few micrometers in diameter.

#### 1.1.1.1 Beads on a String

DNA from eukaryotic nuclei is associated with an equal mass of protein in a highly compacted complex called chromatin. The most abundant proteins associated with eukaryotic DNA are histones, a family of basic proteins present in all eukaryotic nuclei. The five major types of histone proteins - termed H1, H2A, H2B, H3, and H4 - are rich in positively charged basic amino acids, which interact with the negatively charged phosphate groups in DNA. As described below, histones play an important role in packing very long DNA molecules in an orderly way into a nucleus only a few micrometers in diameter.

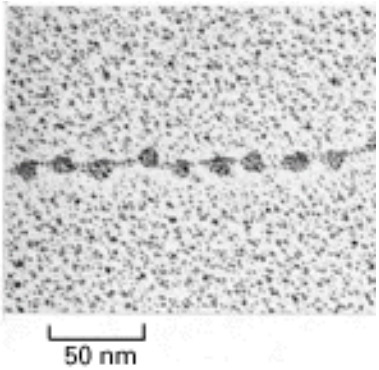


Figure 1.1: **Electron micrograph of nucleosomes**. The nucleosomes form a "beads-on-a-string" structured chromatin. Each nucleosome is separated from the next by a region of linker DNA (adapted from [3])

In 1974 the fundamental packing unit, the nucleosome , was discovered. The nucleosome consists of 146 nucleotide pairs wound slightly less than two times around a specific complex of eight nucleosomal histones (the histone octamer). The histone core is build by two copies of each of the four nucleosomal histones H2A, H2B, H3, and H4. In electron micrographs the nucleosomes give chromatin a "beads-on-a-string" appearance, after treatments that unfold higher-order packing (see figure 1.1). Each nucleosome is separated from the next by a region of linker DNA, which can vary in length from 10 to 80 nucleotide pairs. The nucleosome beads are disc-shaped particles with a diameter of about 11 nm.

#### 1.1.1.2 The 30 nm fiber

In living cells the extended "beads-on-a-string" form of chromatin is rarely present. Chromatin extracted from cells in isotonic buffers, appears as 30 nm fiber in electron micrographs (see figure 1.2). These fibers represent a more condensed state of the chromatin.

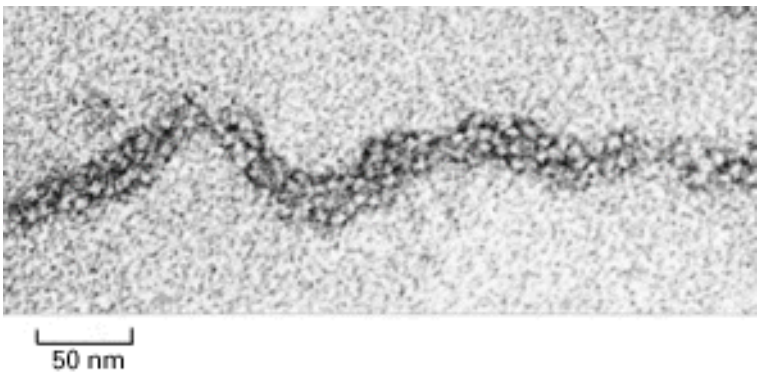


Figure 1.2: **The 30 nm fiber in the electron microscope**. The "beads-on-a-string" are further packed into a 30 nm fiber (figure adapted from [3])

A model for the 30 nm fiber is, that the nucleosomes are packed into a spiral or solenoid arrangement with 6 nucleosomes per turn. Each full turn of the solenoid, thus contains about 1.2 kb of DNA. The histone H1 molecules, are thought to be responsible for pulling nucleosomes together to form the 30 nm fiber, by binding to two adjacent nucleosomes.

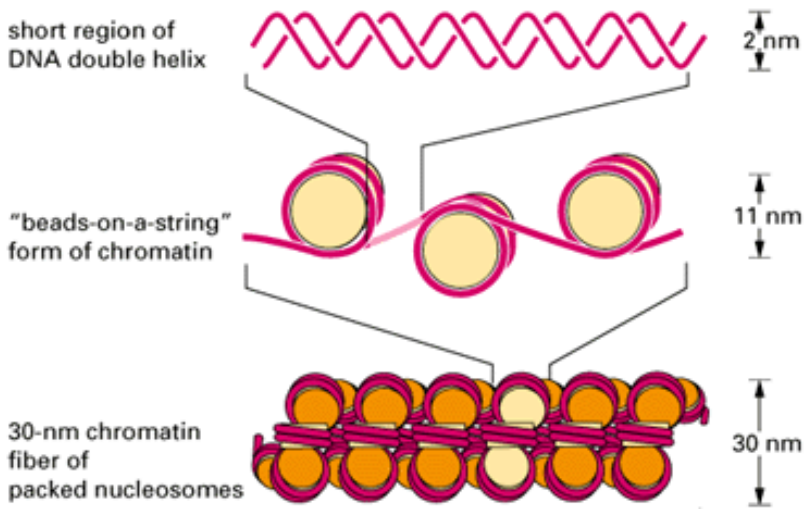


Figure 1.3: **Basic DNA packing levels**. DNA packing levels from the linear DNA double helix to the 30 nm fiber. (Image adapted from [3])

However, models are varying from a highly regular, helical to an irregular folding of nucleosomes. Figure 1.3 summarizes the basic DNA packing levels from the linear double helix to the 30 nm fiber.

### 1.1.2 Higher order DNA packing

A typical human chromosome would have a length of 0.1 cm, if packed only as 30 nm fiber. In this case it would still exceed the size of the nucleus by a factor of 100. The central problem is to arrange the 30 nm fiber in a way that it fits in to the limited space of a nucleus and thereby leaves also adequate space for molecular processes such as transcription and replication [25]. So it is clear that there must exist a higher order of chromatin packing. This higher-order is one of the most poorly understood aspects of chromatin [7]. Its molecular basis is still not understood, but it is believed that this packaging plays a crucial part in the regulation of gene transcription.

In metaphase chromosomes the compaction is extreme. It is difficult to analyze the structure of the complex folding in this most condensed status [46], and it will not be discussed in this work.

There exist different models for the large-scale chromatin structure in interphase chromosomes. Basically they can be divided into two major models, which will be presented below.

#### 1.1.2.1 Loops on a protein scaffold

Back in 1977 Paulson and Laemmli found that, following the removal of the histones, the DNA of interphase chromosomes as well as metaphase chromosomes remains in a highly folded configuration organized by nonhistone proteins. These proteins are believed to represent a central scaffold in mitotic chromosomes [20]. Electron micrographs of histone-depleted metaphase chromosomes from HeLa cells revealed long loops of DNA anchored to the chromosome scaffold. Based on this finding the model for interphase chromosomes was deduced. In this model the DNA fibers form radial helical coiled loops that are attached on their base to the nonhistone protein scaffold, also known as matrix. The DNA interacts with the matrix with specific sites, the "Matrix Association Regions" (MARs) or "Scaffold Attachment Regions" (SARs) [55].

It is believed that heterochromatic regions maintain their condensed metaphase conformation. In contrast, euchromatic regions unfold from the 700 nm structure (metaphase chromatid) and form 200-240 nm fibers that are organized as radial loops of 30 nm fibers. These loops are thought to be more or less compact, depending on the transcriptional activity in the region [25, 46]. A schematic view of the "DNA loops on a protein scaffold" is illustrated in figure 1.4.

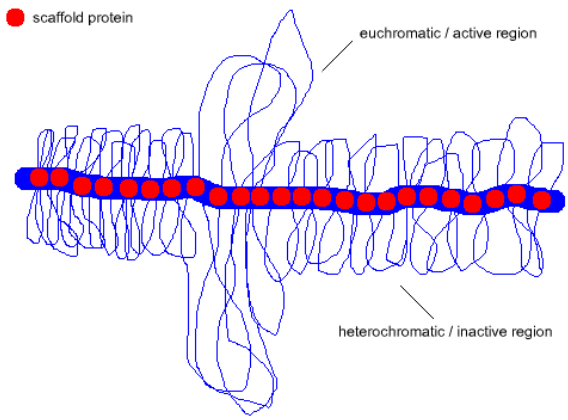


Figure 1.4: **Loop - Scaffold model**. Schematic representation of the loop - scaffold model. DNA fibers form radial coiled loops that are attached on their base to the protein scaffold. Active regions show unfolded loops in contrast to inactive regions.

#### 1.1.2.2 Chromonema fiber model

The second model for higher order chromatin organization is based on electron microscopy observations and proposes, that higher order 30 nm fibers and possibly 10 nm fibers fold into 60-80 nm "chromonema" fibers. The chromonema fibers are then further compacted, either through folding into 100-130 nm chromonema fibers, or through a continuous remodelling process. The larger chromonema fibers are themselves bent, folded and kinked into condensed chromatin masses. Additional condensation over large chromosomal regions - during mitosis - ends up into linear chromatids . In interphase the chromatids are decondensed by progressive unfolding of 100-130 nm chromonema fibers. This decondensation however, seems to be nonsynchronous and there exist more and less condensed regions [6, 19].

There is evidence that the structural organization beyond the 30 nm fiber is dynamic. Studies were performed on artificial tandem arrays that showed large-scale decondensation upon transcriptional activation. Decondensed regions appeared as fibers, which recondensed after inhibition of transcription [28, 38].

This model does not depend on a scaffold to which the DNA is attached and by which the structure is maintained. Supporters of this second model argue that the protein scaffold observed after the removal of histones might be an artefact caused by cross-linking events of nonhistone proteins occurring in vitro.

A schematic view of the chromonema model is shown in figure 1.5.

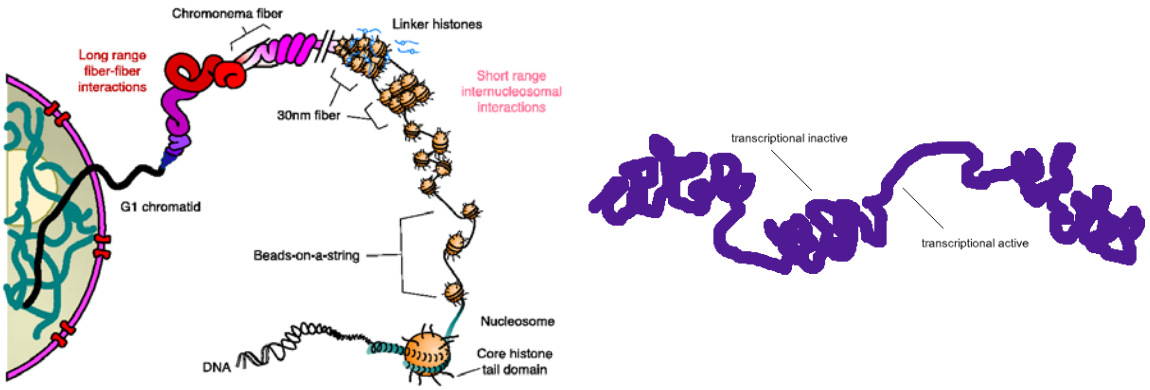


(a) (b)

Figure 1.5: **The chromonema model**

Strings of nucleosomes compose the 30 nm fiber. Further folding and compaction of the 30 nm fiber produces the chromonema fiber (a, taken from [19]). The chromonema fiber shows different levels of compaction, depending on transcriptional activity (b).

## 1.2 Transcription and chromatin

Chromatin plays an important role in regulation of gene expression. The huge amount of DNA compacted into the nucleus of an eukaryotic cell must be accessible to DNA-binding proteins that are involved in transcription . Therefore, regions of the genome that are transcriptionally active have a more open and accessible structure than non-transcribed regions.

Basically, transcription occurs in two steps. 1) Initiation: transcription factors and RNA-polymerase II bind to the promotor-sequence of a gene and set on the synthesis of RNA.

2) Elongation: the polymerase moves along the DNA and synthesizes an RNA transcript. In the past a lot of studies focused on the accessibility of DNA on transcription initiation sites. They revealed local changes in nucleosome structure and histone modifications. For example, histone H1, is depleted at active sites, tails of other histones become actetylated [30]. But not only local changes of chromatin structure occur in transcriptionally active regions. Evidence for this provides the increased nuclease sensitivity of transcribed regions, and microscopic observations of active regions [38, 37, 28], which show large-scale unfoldings of actively transcribed chromatin, rather then localized decondensation.

# Chapter 2

# Objectives

The goal of this project was to predict and identify large scale chromatin decondensations within interphase chromosomes in a natural system.
In previous work, several groups could already show large scale chromatin decondensation [28, 37, 38]. However, these studies were based on artificial tandem arrays integrated into chromosomes rather than on natural sequences. Thus, these systems could only serve as models for large scale chromatin organization and suggest how it might look in a natural system.
In order to find out what the large scale chromatin structure looks like in a natural system an unbiased approach was considered. This approach was divided into two major tasks, which will be described in this section.

## 2.1 Bioinformatics

It was described before [13] that genes with similar functions tend to occur in adjacent positions along a chromosome and are co-expressed. Such groups of correlated adjacent genes appear throughout the genome and show a statistical significant occurrence. More recent studies [9, 33] confirm these findings. These results suggest that these gene clusters may correspond to regions of active chromatin, because opening chromatin for one gene can result in the opening of neighbouring chromatin [18, 36], transcriptional machinery

may access two co-expressed genes more efficiently if they are neighbours than if they are apart.

These results show that a large scale chromatin decondensation could be found in regions of co-regulated and active genes. To identify such regions an analysis of microarray data using bioinformatic methods was considered. The result of the analysis should give predictions of different levels of chromatin compaction on a specific chromosomal region, either in different cell lines or in one cell line under different conditions.

## 2.2 Microscopy: FISH

The second part of this work was the identification of large scale chromatin decondensations using the DNA FISH technique. Based on the results from the microarray analysis, a chromosomal region which is predicted to show changes in chromatin structure/compaction caused by transcription, should be examined by fluorescence microscopy. Fluorescence in situ hybridization makes it possible to visualize single sequences within decondensed interphase chromosomes [21]. Thus it should be possible to use this technique to look at the predicted sequences/regions, and determine if there are differences in chromatin structure between two cell lines.

# Chapter 3

# Methods

## 3.1 Bioinformatics

To discover regions on a chromosome that show differences in their gene expression level in a large scale format, an analysis of public available microarray data was considered.
cDNA microarrays are capable of profiling gene expression patterns of tens of thousands of genes in a single experiment [14]. Thus, it is also possible to monitor the expression of all genes, even all exons along a whole chromosome with this technology. Data sets originating from such experiments are usually hard to handle by conventional methods (data reading, spread sheets), for they can contain the information of tens of thousand of probes across multiple experiments or time points.
Bioinformatic methods can help to deal with the huge amount of data produced by DNA microarray experiments.
In this work a relational database management system (RDBMS) *MySQL* [48] and the programming language *Perl* [47] was used in order to handle, retrieve, store and manage data derived from microarray experiments.
As further analysis tool, BLAST came in use to map and verify DNA sequences.

### 3.1.1 Perl

Perl is a programming language optimized for scanning arbitrary text files, extracting information from those text files, and printing reports based on that information. The language is intended to be practical (easy to use, efficient, complete). Perl can use sophisticated pattern matching techniques to scan large amounts of data quickly. It combines some of the best features of C, sed, awk, and sh, so people familiar with those languages have little difficulty with it. Expression syntax corresponds closely to C expression syntax. Unlike most Unix utilities, Perl does not arbitrarily limit the size of data [47]. Other benefits of Perl are modularity and reusability of already existing code using modules. Extension modules are written in C (or a mix of Perl and C). They are usually dynamically loaded into Perl if and when they are needed, but may also be linked in statically. C extension modules like DBI (3.1.1.1), GD (3.1.1.2) or Chart::Plot (3.1.1.3) which were used for this work, can be found on CPAN [2].
Because of the features of Perl, it was chosen in this work as programming language to develop programs, which deal with the large amount of data coming from the microarray experiments.

#### 3.1.1.1 The DBI module

The DBI (Database Interface) is a database access module for the Perl programming language. It defines a set of methods, variables, and conventions that provide a consistent database interface, independent of the actual database being used. It is a layer of "glue" between an application and one or more database driver modules. It is the driver modules which do most of the real work. The DBI provides a standard interface and framework for the drivers to operate within [8].

**Architecture of a DBI Application:** The API , or Application Programming Interface, defines the call interface and variables for Perl scripts to use. The API is implemented by the Perl DBI extension. The DBI "dispatches" the method calls to the appropriate driver for actual execution. The DBI is also responsible for the dynamic loading of drivers,

error checking and handling, providing default implementations for methods, and many other non-database specific duties. Each driver contains implementations of the DBI methods using the private interface functions of the corresponding database engine. Only authors of sophisticated/multi-database applications or generic library functions need be concerned with drivers. In figure 3.1 a simple schema of an application using the DBI is shown [8].

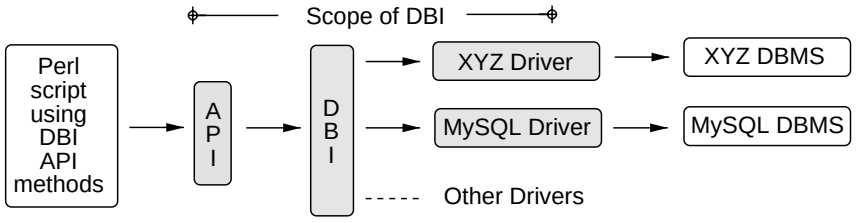


Figure 3.1: **DBI Application Architecture.** Shown is a schema of an DBI application, where the Perl program calls methods from the DBI API. The DBI uses a specific database driver to communicate with the database.

In the Perl applications written for this work, the database driver *DBD::mysql* for the DBI was used to retrieve and store data from the MySQL-database. This driver is available at CPAN.

#### 3.1.1.2 The GD module

The GD module is a Perl interface to Thomas Boutell's gd graphics library [53]. GD allows one to create color drawings using a large number of graphics primitives and output the drawings as PNG files. The gd library allows rapid drawing of images complete with lines, arcs, text, multiple colors, cut and paste from other images, and flood fills, and write out the result as a PNG or JPEG file [4].

#### 3.1.1.3 The Chart::Plot module

Chart::Plot allows one to create images of simple graphs of two dimensional data. It plots multiple data sets in the same graph, each with negative or positive values from independent or dependent variables. Each dataset can be a scatter graph (data are represented by

graph points only) or lines connecting successive data points, or both. Colors and dashed lines are supported. Axes are scaled and positioned automatically, ticks are drawn and labeled on each axis [49]. This Perl module requires the GD module.

#### 3.1.1.4 The GFF module

GFF is a Perl Object base class/module for the General Feature Format (GFF) 3.1.2. It allows one to read, parse and handle data in the GFF format. It provides also the possibility to write GFF files, merging different GFF data sets and sorting GFF features [54].

### 3.1.2 The General Feature Format - GFF

GFF is a format for describing genes and other features, like exons, introns, polyA-sites etc. associated with DNA, RNA and protein sequences.
The GFF format is intended to be easy to parse and process by a variety of programs in different languages. For example, Unix tools like grep, sort and simple Perl and awk scripts can easily extract information out of a GFF file. For these reasons it has a record-based structure, where each feature is described on a single line, and the line order is not relevant [51]. A GFF record is an extension of a basic (name, start, end) tuple (or "NSE") that can be used to identify a substring of a biological sequence. For example, the NSE (ChromosomeI, 2000, 3000) specifies the third kilobase of the sequence named "ChromosomeI".
The most common operations that one typically wants to perform on sets of NSEs and NSE-pairs include intersection, exclusion, union, filtration, sorting, transformation (to a new co-ordinate system) and dereferencing (access to the described sequence). With a suitably flexible definition of NSE "similarity", these operations form a basis for more sophisticated algorithms like clustering and joining-together by dynamic programming.

### 3.1.3 MySQL

MySQL , a popular Open Source SQL database, is developed, distributed and supported by MySQL AB. A database is a structured collection of data. It may contain any information from a simple shopping list to a picture gallery or vast amounts of information like biological data. To add, access, and process data stored in a computer database, a database management system (DBMS ) such as the MySQL Server is needed.
MySQL is a relational database management system (RDBMS ). A relational database stores data in separate tables rather than putting all the data in one big storeroom. This adds speed and flexibility. The tables are linked by defined relations making it possible to combine data from several tables on request. The SQL part of "MySQL" stands for "*Structured Query Language*", the most common standardized language used to access databases [48].

### 3.1.4 BLAST

BLAST (Basic Local Alignment Search Tool) is a tool for sequence similarity searches. It can be used to compare both, protein or DNA sequences. BLAST uses a heuristic algorithm to seek local alignments and is therefore able to detect similarities among sequences, even if they share only isolated regions of similarity [5].
The BLAST program set was downloaded from NCBI (ftp://ftp.ncbi.nih.gov/blast/). For the sequence mapping (see 3.1.8) and verification (see 3.2.1.2) in this work the megablast tool, which makes part of the BLAST tool set, was utilized, because it is optimized for aligning sequences that differ slightly. It is also able to efficiently handle much lager DNA sequences than the traditional blastn program.

### 3.1.5 Microarray data

For an accurate prediction of transcriptional mediated chromatin decondensation it was necessary to have gene expression data that covers a whole chromosome. It was also important, that the genes (probes) on the microarray were annotated and their chromosomal

position was known. Therefore, public available gene expression data from microarray experiments, that meets these requirements, were searched.

The search led to several sources. One of them was the whole-genome mRNA expression data generated for the mitotic cell cycle of *S. cerevisiae* [11]. The disadvantage of the yeast in terms of identifying large scale chromatin structures by fluorescence microscopy, is that the yeast chromosomes are relatively small (largest 2.2 Mbp). In previous studies [28] large scale decondensation of the MMTV array (mouse mammary tumor virus), where the most decondensed arrays had a 50-fold chromatin compaction, could be shown. This construct has a length of $\geq$ 2 Mbp, which is about the size of the largest yeast chromosome, and is build homogeneously by $\geq$ 200 repeats of a 9 Kbp sequence [27]. The detection limit of the light microscope is about 0.4 $\mu$m, that means that a detectable decondensed structure would already require a size of $\sim$60 Kbp and would produce a dot shaped image. It is unlikely that a natural chromosome is as homogeneous in its sequence as the MMTV, thus one could expect a higher compaction rate in decondensed regions. Therefore it may require a size of $\sim$0.5-1 Mbp to see large-scale chromatin decondensations on a natural chromosome and to be able to study its structure. It is unlikely that a good part or even a whole chromosome is transcriptional active in yeast at the same time. To be sure that the structure of an active gene cluster could also be identified and studied by DNA FISH, the decision was made to use data of an organism with larger chromosomes.

A data set which satisfied all the requirements (annotation, probes with known chromosomal positions, whole coverage of a chromosome, large chromosomes) came from an experimental annotation of the human chromosome 22q using microarrays [34]. In this work the authors describe a high-throughput, microarray-based experimental method to validate predicted exons , group the exons into genes by coregulated expression and define full-length mRNA transcripts. Chromosome 22 was the first human chromosome to be completely sequenced and annotated [15]. Shoemaker et. al. designed a single ink-jet microarray to validate the 8,183 exons annotated [15] on chromosome 22q under different experimental conditions. The mRNAs from human cell lines and tissues were fluorescently

labeled with two dyes (cy3 and cy5) and hybridized in pairs to 69 individual chromosome 22 exon arrays. The probes on the exon arrays based on 6,650 Genscan-predicted exon sequences, and 3,381 validated exon sequences [34]. From this set of 10,031 exons 1,848 were identical and thus removed form the pool. For each of the resulting 8,183 exon sequences two 60-mers were selected as probes on the microarray. For exon sequences with 60 or less nucleotides, a single probe consisting of the entire sequence was used. This led to an array with 15,511 60-mers, which covered the whole q-arm of chromosome 22.

#### 3.1.5.1 Gene expression data extraction

The results of the microarray experiment from Rosetta Inpharmatics were downloaded from the company's website [42] as a 220Mb zip archive. It contained a directory for each of the 69 experiments. These directories contained data files for the experiment and the corresponding reversed flour experiments. The expression data in these files were stored in the GEML$^{TM}$ [43] format.

Gene Expression Markup Language (GEML) is an XML file specification for converting DNA microarray and gene expression data into a common format. To extract the needed data from these files a Perl program, which parsed the formatted text and produced tab separated lists as output, was written. The extracted fields were the following: probename, raw and normalized value for the cy3 and cy5 channel, $\log_{10}\frac{cy5}{cy3}$, error of $\log_{10}\frac{cy5}{cy3}$ ($= \sigma_{\log_{10}\frac{cy5}{cy3}}$) and XDEV ($= \log_{10}\frac{cy5}{cy3}/\sigma_{\log_{10}\frac{cy5}{cy3}}$).

The probename consisted of the sequence-contig name, followed by the index (exon count) of the exon in that contig and followed by *_te* for *true exon* or *_pe* for *predicted exon*. The probenames were not unique, because the microarray incorporated two probes (60-mers) for each of the 8,183 exons. To identify a single probe, each probe was given a unique id (*P_ID*) additionally.

#### 3.1.5.2 Error weighted exon expression

Since there were more than one probe (including replicates) per exon it was necessary to calculate an error weighted mean value over all the probes belonging to the same exon,

so that an overall expression value could be obtained. In order to average the multiple probes for one exon with appropriate relative weights, a model for the uncertainties in individual probe measurements was required. Roberts et al. [32] have developed such a model. It was applied to the microarray experiment data. To compute the mean $\log_{10} \frac{cy5}{cy3}$ of an exon, the minimum-variance weighted average was used:

$$w_i = \frac{1}{{\sigma_i}^2} \tag{3.1}$$

$$\bar{x} = \sum_{i=1}^{n} w_i x_i / \sum w_i \tag{3.2}$$

In equation 3.1 $\sigma_i$ is the error of $\log_{10} \frac{cy5}{cy3}$ and in equation 3.2 $x_i$ stands for the $i$-th measurement of $\log_{10} \frac{cy5}{cy3}$, $n$ is the number of probes.

### 3.1.6 Sequence data

The microarray study was based on the analysis version of human chromosome 22 published in Nature in December 1999 [15]. The spotted probes on the microarray were chosen according to the GFF (3.1.2) files for the q-arm of chromosome 22. The files for known [16] and predicted [17] genes are available from the Sanger Centre. These GFF files together contained information about 10,031 exons . 1,848 of them had coordinates identical to those of other exons and were removed form the sequence pool for the microarray.

To extract the basepair coordinates of the probes it was necessary to parse the GFF files. Therefore a Perl program, that made use of the GFF Perl module 3.1.1.4, was written.

#### 3.1.6.1 Exon extraction

The downloaded archives for the known and predicted genes contained a GFF file for each sequence-contig of human chromosome 22. First the files for the known genes were loaded and the GFF features labeled as *exon* were parsed, then the same was done with the files for the predicted genes, with the exception that here the GFF features labeled

as *CDS* were extracted. The acquired features were then merged and sorted ascending according to the start positions of the extracted exons. The obtained data included the contig name, the start and end base position of the exon and the DNA-strand of the coding sequences. Each exon found this way was given a unique id (*E_ID*). Furthermore the index number of the exon (*Exon_Nr*) on a particular contig was determined simply by counting the exons on it. The length of an exon was calculated by subtracting the start position from the end position and adding 1. The Perl program produced a sorted and tab separated list of entries containing 10,031 annotated exons. Such an entry contained the following data fields:

| E_ID | contig | Exon_Nr | start base | end base | DNA-strand | exon length | exon type |
|---|---|---|---|---|---|---|---|

**Explanation:**

- E_ID: represents a unique ID for each exon
- contig: represents the sequence-contig on which the exon is located
- Exon_Nr: is the index (exon count) of a exon on the specified contig
- start base: is the number of the first base of a exon on chromosome 22q
- end base: is the number of the last base of a exon on chromosome 22q
- DNA-strand: is the DNA strand on which the coding sequence of a exon is located
- exon length: is the length of an exon in base pairs
- exon type: determines the type of the exon (predicted / known)

#### 3.1.6.2 Gene extraction

For extracting the known and predicted genes from the GFF files a Perl program was written. It parsed the GFF features labeled as *sequence*, merged the list of the acquired predicted and known genes, and sorted them ascending according to their start base position on the chromosome. The output produced by this program gave a list containing the following extracted gene feature fields:

| G_ID | contig | Gene_Nr | start base | end base | DNA-strand | gene length | gene name | description | gene type |
|---|---|---|---|---|---|---|---|---|---|

**Explanation:**

- G_ID: represents a unique ID for each gene
- contig: represents the sequence-contig on which the gene is located
- Gene_Nr: is the index (gene count) of a gene on the specified contig
- start base: is the number of the first base of a gene on chromosome 22q
- end base: is the number of the last base of a gene on chromosome 22q
- DNA-strand: is the DNA strand on which the coding sequence of a gene is located
- gene length: is the length of a gene in base pairs
- gene name: is the name of the coding sequence given in the GFF file
- description: is a short description of the coding sequence
- gene type: determines the type of the gene (predicted / known)

These lists could easily be imported into a relational database.

### 3.1.7 The database

To establish a connection between the expression data from the microarray and the positions of the single probes on the chromosome, a relational database model was developed.

#### 3.1.7.1 Sequence data

The known and predicted exons of the q-arm of the chromosome (22q) were extracted from the GFF files and led to the described lists.
A table for the sequence-contigs was created, where each of the contigs was entered with a unique id *C_ID*, the name of the contig *Contig*, the start and end base and its length. A second table held the information about the exons extracted from the GFF files (see

3.1.6.1). The table was linked to the contig table over the contig id *C_ID*, so that for each exon the sequence-contig could be identified by following this link. The data fields resulting from the gene extraction (see 3.1.6.2) were entered into their own table. This table was also connected with the *C_ID* to the contig table. The connection between genes and exons was established by a "map table", where for each exon id (E_ID) the corresponding gene id (G_ID) was entered.

#### 3.1.7.2 Gene expression data

The descriptions of the 69 experiments were put into a table, where each experiment got a unique id (*X_ID*). The experiments were done with two differently designed slides, so that the information about the used slide (*Slide_Set*) was entered as well.
Each probe from the two different slides was extracted from the GEML$^{TM}$ files and entered into a table with a unique id (*P_ID*), the slideset id (*Slide_Set*) and the feature number (*F_ID*) on the microarray. The connection between exons and probes was realized through the exon id *E_ID*, which links a probe to an exon in the *Exons* table.
The expression data, which resulted from the microarray experiments, was entered in its own table. It included the following fields for each probe: raw and normalized values for both channels (cy3, cy5), $\log_{10} \frac{cy5}{cy3}$, $\sigma_{\log_{10} \frac{cy5}{cy3}}$ and XDEV. These values could be linked through the probe id *P_ID* to the corresponding probe in the *Probes* table and through the *X_ID* to the experiment from which the data originate. The same schema was used for the reversed fluor experiments.
Since there were multiple probes for a single exon on the microarrays, the average (mean) of the intensities of all probes on an exon were calculated and listed in the table *Exon_Expression*. Also an error weighted $\log \frac{cy5}{cy3}$ (see 3.1.5.2) of all probes belonging to an exon was entered there.
In figure 3.2 a schema of the database layout is shown.

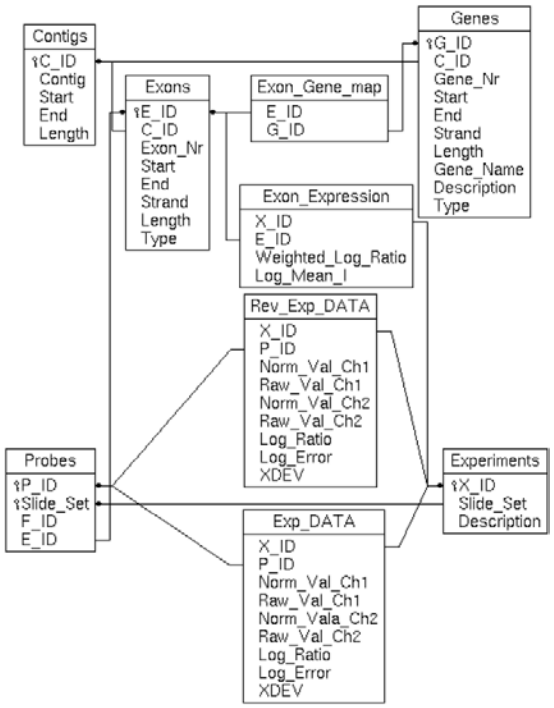


Figure 3.2: **Data model**. shown are the tables of the database, connecting lines represent constrains

### 3.1.8 The scoring system

In order to find regions on the chromosome where there are significant differences in gene expression between two different cell lines, a scoring system was developed.

The start and end (borders) of such regions were determined by a set of 22 bacterial artificial chromosomes (BACs ), that have previously been mapped cytogenetically by FISH to chromosome 22 (see 3.2). This BAC set is part of the FISH-mapped BACs from the "Cancer Chromosome Aberration Project" (Ccap) [52, 10]. In this project a high-resolution fluorescence in situ hybridization (FISH) mapping of colony-purified BAC clones, spaced at 1 to 2 Mbp intervals across the entire genome, was done.

The available sequences (BAC-end sequences, STS, entire sequences) of the BACs were

downloaded from GeneBank (http://www.ncbi.nlm.nih.gov) and mapped to the sequence of the q-arm of human chromosome 22 [15] . The mapping was done with the megablast program from NCBI (see 3.1.4).

With the scoring system the 21 resulting regions (each defined by the start- and end position of two neighboring BACs) were scored with regard to the difference in the expression levels, the number and the length of the genes within such a region. The score is influenced by the mean $\log_{10}$ of the expression ratio of the known and predicted exons on a gene in the region, the mean $\log_{10}$ of the intensities of the spots of the exons on a gene on the microarray, and the lengths of the different genes in the region. The first two parameters take the difference in the expression level into account. The length of a gene determines the size of the DNA piece over which the RNA-polymerase passes during transcription, and thus the size of potential open chromatin.

#### 3.1.8.1 The algorithm

For the scoring a Perl-program was written. It fetched the expression data, using the DBI (see 3.1.1.1), from the relational database system (MySQL) where the results of the microarray experiments were stored. The program incorporated the following algorithm :

**for all** *genes* in *region* **do**

  **for all** *exons* on *currentgene* **do**

    **if** $\log_{10} \frac{cy5}{cy3} \geq ratio\_threshold$ AND $\log_{10} spot\_intensity \geq intensity\_threshold$ **then**
      $upreg\_gene\_score = upreg\_gene\_score + ((\log_{10} spot\_intensity + 2) * \log_{10} \frac{cy5}{cy3})$
      $increaseupreg\_gen\_countby1$
    **else if** $\log_{10} \frac{cy5}{cy3} \leq -ratio\_threshold$ AND $\log_{10} spot\_intensity \geq intensity\_threshold$ **then**
      $downreg\_gene\_score = downreg\_gene\_score + ((\log_{10} spot\_intensity + 2) * \log_{10} \frac{cy5}{cy3})$
      $increasedownreg\_gen\_countby1$
    **end if**
  **end for**
  $upreg\_gene\_score = upreg\_gene\_score/upreg\_gen\_count$
  $downreg\_gene\_score = downreg\_gene\_score/downreg\_gen\_count$
  **if** $upreg\_gene\_score + downreg\_gene\_score \geq (intensity\_threshold + 2) * ratio\_threshold$ **then**
    $gene\_score = (upreg\_gene\_score + downreg\_gene\_score) * gene\_length$
  **end if**
  **if** $upreg\_gene\_score + downreg\_gene\_score < (intensity\_threshold + 2) * -(ratio\_threshold)$ **then**
    $gene\_score = (upreg\_gene\_score + downreg\_gene\_score) * gene\_length$
  **end if**
  $score = score + gene\_score$
**end for**

**Explanation:** Each exon on a gene which showed an expression ratio ($\log_{10} \frac{cy5}{cy3}$) and a spot intensity on the microarray ($\log_{10} spot\_intensity$) beyond certain thresholds was considered as significantly up- or downregulated. For the expression ratio thresholds (ratio_threshold) 0.3 and -0.3 was used in this work - this represents a 2-fold up- or downregulation of the exon in one cell line. The threshold for the spot intensity (intensity_threshold), which correlates to the amount of RNA, was -0.7. Below this threshold errors tend to increase rapidly because spot intensities are not sufficiently above background intensity, therefore the values were not considered reliable [26].
For each of the up- or downregulated exons on a gene, an intermediate score (upreg_gene_score, downreg_gene_score) was calculated. For doing this the values for the intensities were first corrected by 2, to always get positive values. Then the corrected intensity value was multiplied by the expression ratio value. These intermediate scores for the upregulated exons were summed up and divided by the number of the exons on the gene. The same was done for the downregulated exons. These two mean values (upreg_gene_score and downreg_gene_score) were then summed up and multiplied by the length (in bases) of the gene. This resulted in another intermediate score (=gene_score) which represents a score for a single gene. The score for a gene was only considered as significant if the sum $upreg\_gene\_score + downreg\_gene\_score$ was bigger or smaller then the threshold of $(intensity\_threshold + 2) * ratio\_threshold$ or $(intensity\_threshold + 2) * -(ratio\_threshold)$ respectively. The significant gene scores of a region were then summed up to come to the total score for the region.

### 3.1.9 Visualization of exon expression

To visualize the expression of the exons in the 21 different regions on human chromosome 22, a scatter plot for each region was created using the Chart::Plot, GD and DBI Perl modules.
The $\log_{10}$ of the expression ratio for each exon in a particular region was plotted against the $\log_{10}$ of the mean intensity of each exon. The resulting plots illustrate an expression

profile for each region. The study of these profiles in combination with the calculated scores helped to find regions of interest.

## 3.2 Microscopy: FISH

With the above described methods it was possible to find transcriptional highly active, and thus interesting regions on human chromosome 22. These regions should also show a different structure in the chromatin, compared to a region with low transcriptional activity [46, 19]. The structure of the chromatin in such a region should be visualized with the help of fluorescence microscopy, using the DNA FISH method.

**In situ hybridization** (ISH ), is a method of localizing, either mRNA within the cytoplasm or DNA within the chromosomes of the nucleus, by hybridizing the sequence of interest to a complementary strand of a nucleotide probe. Normal hybridization requires the isolation of DNA or RNA, separating it on a gel, blotting it onto nitrocellulose and probing it with a complementary sequence.

The basic principles for in situ hybridization are the same, except one is utilizing the probe to detect specific nucleotide sequences within cells and tissues. It is presently used by many laboratories for diagnosis of infectious diseases and cytogenetic analyses, as well as for basic cell biology research to study structural and dynamic properties of tissues, cells, and subcellular entities [23].

Probe sequences can be labeled with isotopes, but an increasing number of groups have turned to nonisotopic in situ hybridization. It is faster, has a greater resolution, and provides many options to simultaneously visualize different targets by combining various detection methods [41]. The most popular ISH protocol utilizes fluorescence detection and is therefore also known as FISH.

Nonisotopic labels include enzymes, haptens such as biotin or digoxigenin, and fluorochromes. Usually, FISH is performed with biotinylated or digoxigenin-labeled probes

detected via fluorochrome-conjugated detection reagent, such as an antibody, or hapten-specific reactive compounds, such as avidin or streptavidin when biotin is incorporated. A flowchart of the steps in a FISH experiment is shown in figure 3.3.

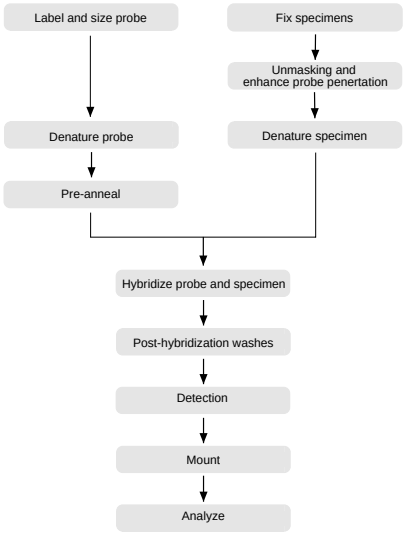


Figure 3.3: **FISH flowchart**. The diagram illustrates the basic steps required for FISH in a temporal sequence

In this section the principal steps that were performed for the DNA FISH will be described. The bioinformatic analysis revealed a region in which three different cell lines showed different gene expression levels (4.1.4). One of them had a very high, one a medium and the last a very low expression in one and the same region of human chromosome 22. A region was determined by two BACs on each end of it (see 3.1.8). To see if transcriptional activity leads to changes in the chromatin structure, one could make probes for the entire region, hybridize them to it, and examine the structure by fluorescence microscopy. However, this would require a lot of foregoing efforts, because for every probe one has to test if DNA-FISH is feasible. It has to be checked, if the probe hybridizes to the right chromosome and the right position on it. Probes that hybridize to multiple positions or chromosomes would lead to wrong results.

For this reason the FISH-mapped BACs from the Ccap project [52, 10] were used, for they were already proofed to be accurate probes for FISH experiments and they can be

purchased from ResGen (Invitrogen Corporation). The BACs covered just the beginning and the end of a region, so that for identifying changes in the chromatin structure, such as decondensation and recondensation, the distance between the two has to be measured. In case of a large scale decondensation of the chromatin, caused by transcription, one would expect an increased distance between the two BACs. In the cell line for which the microarray analysis revealed a low transcriptional activity, a condensed state of the chromatin is predicted, thus the distance between the two BACs at the ends of the region should be smaller.

Lawrence and colleges [22] could already show that it is possible to hybridize two probes, spaced by ∼1Mbp, to an interphase chromosome and produce two distinct fluorescent signals, of which the distance can be measured. This gave confidence that this approach may have success in terms of identifying changes in large-scale chromatin structure.

To test if open structures are caused by transcriptional activity, the cells were treated with 5,6-dichloro-1-$\beta$-D-ribofuranosylbenzimidazole (DRB ), a protein kinase inhibitor that blocks the transition from polymerase II initiation to elongation [12]. The chromatin structure of the DRB treated cells was then studied by DNA FISH.

### 3.2.1 The probe

As probes for the DNA FISH, two BACs flanking the region of interest were used. They were purchased from ResGen (Invitrogen Corp.). The BACs made part of the clone set from the Ccap FISH-mapped BACs for human chromosome 22 (cat. no. MB11200). The insert DNA from human chromosome 22 was cloned into the vector pBACe3.6 (figure 3.4) and transformed into the host strain *E. coli DH10B*. The BAC library was supplied in 96 well microtiter plates as glycerol stocks in Laura Bertani (LB) media with chloramphenicol (12.5 $\mu$g/ml).

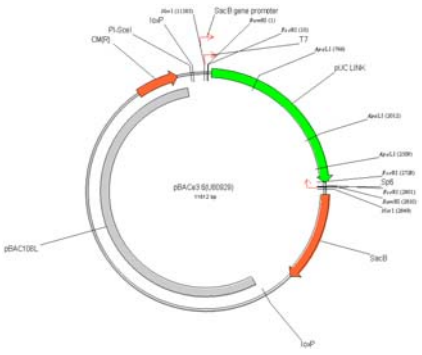


Figure 3.4: **BAC vector**. Shown is a map of the pBACe3.6 vector. Inserts are cloned between t7 and sp6.

#### 3.2.1.1 BAC isolation

For the preparation of the DNA FISH probes it was necessary to obtain single colonies of the BAC clones. In order to achieve this, an ONC of each BAC clone was cultivated in 5ml LB medium with 12.5 $\mu$g/ml chloramphenicol. The ONCs were streaked out on separate LB agar plates containing 12.5mg/ml chloramphenicol. From each plate a single colony was picked and streaked out making a short streak on a new plate. This new plate was the master plate for all of the following work, it contained every single BAC clone. Additionally a glycerol culture (see A.2) of each BAC on the master plate was established.

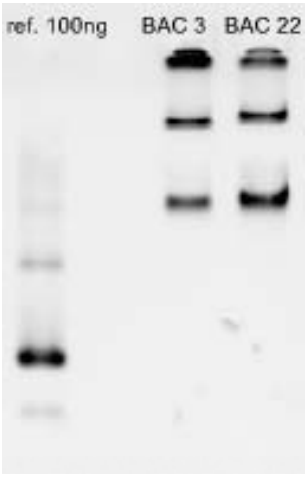


Figure 3.5: **Agarose gel**. Shown is the 1% agarose gel for the DNA yield determination, ref. = reference DNA

From the colonies on the master plate the plasmids (BACs) were isolated using the QIAGEN Large-Construct Kit (QIAGEN Inc., Valencia, CA, USA). The resulting DNA was redissolved in 100$\mu$l $H_2O$. To get the yield of the isolated plasmid DNA , the DNA concentration was determined by a quantitative analysis on a 1% agarose gel, where the intensities of the bands with unknown concentration were compared to a reference DNA with known concentration. The result of this analysis gave a concentration of $\sim$300ng/$\mu$l for both BACs (22, 3) and is shown in figure 3.5.

#### 3.2.1.2 BAC verification

To make sure that the right BACs were isolated, the two BACs were sent to a company (MWG-Biotech, Inc., High Point, NC, USA) where they were end-sequenced. The sequences were then verified by comparing them with the sequence of human chromosome 22 using the BLAST tool (3.1.4).

#### 3.2.1.3 Biotin-Nick translation

To generate biotin labeled probes a biotin nick translation [31] was performed using the Biotin-Nick Translation Mix from Boehringer Mannheim (cat. no. 17452824).

The translation mix contains DNase I, which has the ability to introduce randomly distributed nicks into DNA. The second enzyme - *E. coli* DNA polymerase I - in the mix, synthesizes DNA complementary to the intact strand in a 5' $\longrightarrow$ 3' direction using the 3'-OH termini of the nick as primer. This enzyme has also a 5' $\longrightarrow$ 3' exonucleolytic activity, which simultaneously removes nucleotides in the direction of synthesis. Because the mix contains biotin labeled dUTP, dATP, dCTP, dGTP and dTTP the nicked strand is replaced sequentially by these nucleotides. Thus the unlabeled DNA turns into newly synthesized biotin labeled DNA. For the DNA FISH the length of probe molecules is critical for probe diffusion and hybridization to the specific target sequence. For successful hybridization the DNA probe must be sufficiently nicked in the reaction to produce fragments of ∼200-500 nucleotides [1, 40, 24]. Fragments larger than 500 nucleotides tend to stick to the glass surface and not to penetrate the cells efficiently resulting in an increased background. Too small probes tend to bind nonspecifically and to rehybridize so that a smaller amount of probe can hybridize to the target DNA, leading to poor hybridization efficiency and sensitivity [1]. Therefore, the size of the fragments was checked after the labeling reaction (90 min.) by gel electrophoresis using a 1% agarose gel. The gel is shown in figure 3.6. The left lane is a 1kb ladder which served as reference to estimate the size of the fragments in the lanes next to it. The numbers next to the first lane, represent

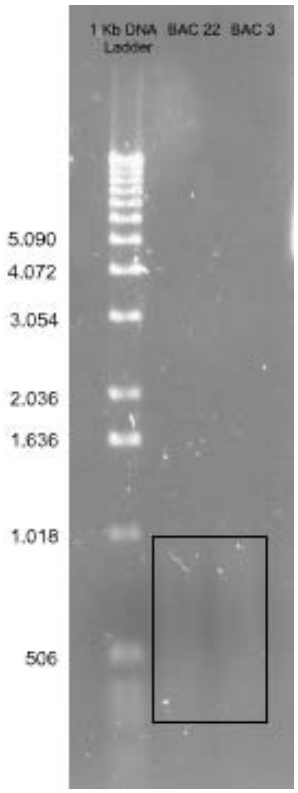


Figure 3.6: **Agarose gel**. 1% agarose gel for fragment size control. Numbers show the size of the bands in base pairs

the size of the bands. The light smear in the box represents the fragment distribution. As one can see, the size of the fragments ranges from ∼1000 to 300 bases, therefore the nick translation was extended for 15 minutes in order to obtain fragments in the range of ∼200-500 nucleotides. After the labeling reaction the probe DNA was precipitated and redissolved in 20$\mu$l $H_2O$.

#### 3.2.1.4 Probe preparation for in situ hybridization

After the biotin-nick translation further preparation steps are required.
Large probes often contain interspersed repetitive sequences (IRS ) that can cause background staining, because of the wide distribution of these sequences throughout the genome. To prevent binding of labeled IRS within the probe to sequences other than the targeted locus, chromosomal in situ suppression hybridization (CISS ) [24] was performed. In this method competitor DNAs , COT-1 from Invitrogen (Invitrogen Corporation, Carlsbad, California 92008, cat. no. 15278-011) and salmon sperm DNA (Invitrogen, cat. no. 15632-011), are used in a preannealing step. COT-1 DNA is obtained from human placental DNA and is rich in repetitive sequences, which can mask the IRS on the probe. Salmon sperm DNA shares certain repetitive DNA elements in common with human DNA. It also prevents nonspecific binding of the hybridization-probe to the glass surface of the coversilp used for FISH. Salmon sperm DNA acts also as carrier.
Briefly, biotinylated DNA (150 ng), COT-1 DNA (5 $\mu$g) and salmon sperm DNA (7 $\mu$g) were combined in the hybridization solution and precipitated with $\frac{1}{10}$ vol. 3M sodium acetate pH 5.2 and 2 vol. abs. EtOH at $-80°$C. After precipitating, the DNA was washed with 70% EtOH, dried and redissolved in 2.5 $\mu$l formamide and 1 $\mu$l $H_2O$ at 37°C for 20 minutes. 0.5 $\mu$l 20xSSC and 1 $\mu$l 25% dextran sulfate were added. The hybridization cocktail with final concentrations of 50% formamide and 2xSSC determines the stringency of denaturation and renaturation. Stringency can be increased by either raising the temperature, increasing the concentration of formamide, or decreasing the number of monovalent cations (lowering the SSC concentration).
The probe was denaturated for 10 minutes at 85°C and prehybridized for 20 minutes at

37°C before applying it to a separately denatured specimen (see 3.2.2.6).

## 3.2.2 The specimens

The bioinformatic analysis revealed a region on human chromosome 22, in which three cell lines showed a significant difference in their gene expression (see 4.1.4). This region was flanked by two BACs (22, 3), which were used as probes (see 3.2.1). The cell line K-562 had the highest expression level, Raji had the lowest and Jurkat was in between of K-562 and Raji. The region should therefore show different levels of chromatin compaction in these cell lines.

### 3.2.2.1 Cell cultures

The three cell lines were ordered from ATCC (American Type Culture Collection, Manassas, VA, USA) and cultured according to the procedures described in the product information sheet that comes with the cell lines.
Briefly, for K-562 (cat. no. CCL-243) the Iscove's modified Dulbecco's medium with 4 mM L-glutamine that is modified by ATCC to contain 1.5g/L sodium bicarbonate (cat. no. 30-2005) was used. For Raji (cat. no. CCl-86) and Jurkat (cat. no. TIB-152) the growth-medium was RPMI 1640 with 2mM L-glutamine that is modified by ATCC to contain 10mM HEPES, 1mM sodium pyruvate, 2.4 g/L glucose and 1.5 g/L sodium bicarbonate (cat. no. 30-2001). The medium was supplemented with 10% fetal bovine serum (FBS) and 1% Penicillin/Streptomycin. The cells were grown in 75 $cm^2$ culture flasks (containing 12 ml of medium) at 37°C in a 5% $CO_2$ in air atmosphere. The cultures were maintained by removing 6 ml of the culture suspension and addition of fresh medium of the same volume. This was done on a daily basis.

### 3.2.2.2 Preparation of coverslips

For in situ hybridization, the cells of 6 ml cell suspension were collected by centrifugation (10 min. 800 rpm) and resuspended in 1 ml of fresh medium. 60 $\mu$l of this suspension were

applied onto poly-L-lysine coated coverslips (BD Biosciences, Bedford, MA, USA, cat. no. 354085) and incubated for 1 hour at 37°C. During this incubation the cells attached to the coated coverslip. For the DRB treatment, 100 $\mu$g/ml DRB (Calbiochem, San Diego, CA, USA, cat. no. 287891) was added to the cell suspension before incubation.

#### 3.2.2.3 Cell fixation

To study the structure of chromosomal regions within nuclei by in situ hybridization, it is mandatory that cells retain as much as possible of their in vivo morphology [45, 44, 24]. For preservation of the three-dimensional structure a fixation was performed with paraformaldehyde . It has been shown, that such a fixation has a high degree of preservation of the spatial arrangement of $\sim$1 Mbp chromatin domains [35].
The coverslip with the attached cells was shortly rinsed with PBS (without Ca and Mg = PBS$^{--}$) to wash away the medium. After this washing step the cells were fixed by incubating them in 3.5% paraformaldehyde in PBS$^{--}$ at room temperature for 15 minutes.

#### 3.2.2.4 Cell permeabilization

To enable labeled probes to enter the cell nucleus, it is necessary to permeabilize the cells. This was achieved by a treatment with 0.5% Triton X-100 in PBS$^{--}$. After the fixation step, the cells were washed 2 x 5 minutes with PBS$^{--}$ and incubated for 10 minutes at room temperature in the Triton X-100 solution. At low concentrations the detergent efficiently solvates cellular membranes without disturbing protein-protein interactions.

#### 3.2.2.5 RNase treatment

After permeabilizing, the cells were washed 3 x 5 minutes with PBS$^{--}$. To prevent hybridization of the probe with RNA in the cells, the RNA was digested with RNase. The coverslip was incubated for 20 minutes in a 25 $\mu$g/ml RNase in PBS$^{--}$ solution at room temperature, and washed 3 x 5 minutes with PBS$^{--}$.

#### 3.2.2.6 DNA denaturation

The DNA within paraformaldehyde-fixed cells is denatured by heat in formamide . This procedure produces homogeneously distributed single-stranded DNA.
Before denaturing, the cells were incubated for 1 minute in a denaturation buffer (70% formamide in 2xSSC). Then the coverslip was placed upside-down on a preheated (85°C) slide with a drop of the denaturation buffer on it, and denatured at 85°C. The temperature and duration of the denaturation for the three different cell lines was determined by trying different combinations of time and temperature, and by checking the amount of fluorescence signals after hybridization with the probe. With the optimal condition $\geq$90% of the cells on the coverslip had signals. For Raji and Jurkat the best condition was a temperature of 85°C and a duration of 5 minutes. For K-562 a duration of 3.5 minutes at 85°C was sufficient for the denaturation.
The cells were dehydrated for 4 minutes in 70% EtOH, 4 minutes in 90% EtOH and 4 minutes in absolute EtOH. After that the coverslip with the cells was air-dried.

### 3.2.3 Hybridization

During the hybridization , the probe penetrates the cells and anneals to the complementary sequence on the denatured chromosome. The stringency of the annealing is determined by the composition of the hybridization cocktail (see 3.2.1.4).
The prepared probe (see 3.2.1.4) was applied to a slide, the coverslip with the denatured cells (see 3.2.2.6) was placed upside-down onto the probe and sealed with rubber cement. The hybridization was performed at 37°C in a moist chamber for $\sim$16 hours.
Posthybridization washes remove the nonspecifically bound probe and thus reduce the background staining. Furthermore, the stringency of the FISH can be adjusted by posthybridization washes. Therefore the coverslip was washed as follows after hybridization: 2 x 15 min. in 50% formamide in 2xSSC at 45°C, 10 min. in 0.1xSSC, 10 min. in 2xSSC, 5 min. with 4xSSC.

### 3.2.4 Detection

To detect the hybridized labeled probe, the coverslip was incubated for 45 minutes with 5 $\mu$g/ml NeutrAvidin-Tetramethylrhodamine (Molecular Probes, Eugene, OR, USA, cat. no. A-6373) in 4xSSC, 0.1% BSA and 0.01% Tween 20 (blocking solution).
Avidin has a high affinity for biotin and thus it binds to the hybridized biotinylated probe. It is conjugated to tetramethylrhodamine, which absorbs light at a wavelength of 555 nm and emits fluorescence at 580 nm. The blocking solution prevents nonspecific binding of avidin [21].
The coverslip was washed once for 10 minutes in 4xSSC with 0.1% Tween 20, twice in 4xSSC for 10 minutes and once for 10 minutes in 2xSSC. After that it was placed into $PBS^{--}$, where it could be stored at 4°C for several days.
The samples were stained with the DNA fluorochrome DAPI (diamino phenylindole) at a concentration of 0.2 $\mu$g/ml. The DNA FISH coverslips were examined on a Leica DMRA upright microscope with a Leica 100x 1.3 NA oil immersion objective. Images were collected with a Photometrics Sensys CCD camera with binning of one. This configuration led to a resolution of 0.067 $\mu$m per pixel.

### 3.2.5 Measurements

To identify large scale chromatin decondensations, the distance between the two hybridized probes was measured (see 3.2). The measurements were done with the MetaMorph Offline Version 4.6rs program package (Universal Imaging Corporation, Downingtown, PA, USA).
For each hybridization experiment, images of $\sim$50 randomly selected cells were acquired using an exposure time of 4 seconds. The background in the nuclei was subtracted and the distance between the signals of the two BACs were measured by drawing a line from the end of the first BAC to the end of the second. The number of the pixels of the resulting line was directly transformed into $\mu$m by multiplying them by 0.067. The data were entered into a spreadsheet, for further analysis.

Individual BACs were measured, after background correction, by drawing a line that follows the shape of the signal.

# Chapter 4

# Results

## 4.1 Bioinformatics

The first aim of this work was to find transcriptional highly active regions on a chromosome in a natural system. In order to find such regions, an analysis of DNA microarrays using bioinformatic methods was considered. In this section the results of this unbiased approach are shown.

### 4.1.1 Microarray data

The search for public available microarray data, which covers an entire chromosome, revealed a dataset that was produced by Shoemaker et. al. [34]. In this work the authors used a microarray- based experimental method to validate predicted exons on human chromosome 22. 8,183 annotated exons were monitored under different conditions. Specifically, mRNAs from human cell lines and normal and diseased tissues were fluorescently labeled with two different colors and hybridized in pairs to 69 individual chromosome 22 exon arrays.

The data was imported into a relational database and the expression data of each exon was linked to a sequence position on the chromosome (see 3.1.7). The sequence positions of the exons were extracted from GFF files, which contain the annotation of human chro-

mosome 22 published by Dunham et. al. [15]. This connection between gene expression and chromosomal positions made it possible to analyze a specific region regarding its transcriptional activity across 69 experiments.

### 4.1.2 Region localization through BAC mapping

The regions were predefined by a set of 22 BACs that were FISH-mapped in the Ccap project (see 3.1.8, 3.2). These BACs were located on human chromosome 22 and spaced by 1-2 Mbp. In order to determine their exact location on the q-arm of the chromosome, the available BAC sequences were aligned to the q-arm sequence with the megablast tool. Table 4.1 contains the resulting regions. A region is determined by the start of its upstream and the end of its downstream located BAC:

Table 4.1: Regions flanked by BACs

| Start bp | End bp | Start BAC id | End BAC id | Start clone | End clone |
|---|---|---|---|---|---|
| 1733357 | 3211000 | 1 | 2 | CTA-115F6 | CTA-154H4 |
| 3211000 | 4467680 | 2 | 22 | CTA-154H4 | CTA-433F6 |
| 4322673 | 6100000 | 22 | 3 | CTA-433F6 | CTA-526G4 |
| 6100000 | 7980139 | 3 | 4 | CTA-526G4 | CTA-322B1 |
| 7903301 | 9241971 | 4 | 5 | CTA-322B1 | CTA-221G9 |
| 9139585 | 11156420 | 5 | 6 | CTA-221G9 | CTA-992D9 |
| 11001274 | 13171363 | 6 | 7 | CTA-992D9 | CTA-57G9 |
| 13057573 | 15206259 | 7 | 8 | CTA-57G9 | CTA-99F11 |
| 15206109 | 17005055 | 8 | 9 | CTA-99F11 | CTA-415G2 |
| 16875099 | 18083300 | 9 | 10 | CTA-415G2 | CTA-221H1 |
| 18080632 | 20080711 | 10 | 11 | CTA-221H1 | CTA-212A2 |
| 19867959 | 21310453 | 11 | 12 | CTA-212A2 | CTA-390B3 |
| 21218047 | 22908985 | 12 | 13 | CTA-390B3 | CTA-150C2 |
| 22707843 | 24525531 | 13 | 14 | CTA-150C2 | CTA-229A8 |
| 24402975 | 25901303 | 14 | 15 | CTA-229A8 | CTA-250D10 |
| 25680409 | 28333919 | 15 | 16 | CTA-250D10 | CTA-397C4 |
| 28285673 | 29214699 | 16 | 17 | CTA-397C4 | CTA-268H5 |
| 29025867 | 31250590 | 17 | 18 | CTA-268H5 | CTB-109B5 |

*continued on next page*

| *continued from previous page* | | | | | |
|---|---|---|---|---|---|
| Start bp | End bp | Start BAC id | End BAC id | Start clone | End clone |
| 31239039 | 32340422 | 18 | 19 | CTB-109B5 | CTA-299D3 |
| 32249687 | 33334371 | 19 | 20 | CTA-299D3 | CTA-722E9 |
| 33252951 | 34425742 | 20 | 21 | CTA-722E9 | CTA-799F10 |

### 4.1.3 Scoring system

In order to find regions on the chromosome, which show big differences in gene expression in one of the 69 microarray experiments, a scoring system was developed (see 3.1.8). With the scoring system it was possible to calculate a score for each region across the 69 experiments. The score is influenced by the exon expression ratio, the mean intensity of all probes belonging to an exon and the number and length of the genes in a specific region. The first two parameters take the difference in the expression level into account. The number and length of the genes in a specific region determine the size of the DNA piece over which the RNA-polymerase passes during transcription, and thus the size of potential open chromatin.

### 4.1.4 Regions with potential chromatin decondensation

The scoring system revealed the region 22q11.21-22a that reached high scores in the comparison of the cell lines K-562 versus Jurkat and Jurkat versus Raji . The start of the region is located 4.3 Mbp downstream from the centromere on the q-arm of the chromosome and its length is about 1.7 Mbp. The BAC at the start of the region was BAC 22 (clone id CTA-433F6), the one at the end was BAC 3 (clone id CTA-526G4). A list of the annotated genes in the region can be found in the appendix B.
In this region, K-562 has a higher gene expression compared to Jurkat. In the second experiment (Jurkat versus Raji) Jurkat has the higher transcriptional activity. This result leads to the conclusion, that in this specific region K-562 shows a high, Jurkat an intermediate and Raji a low and activity. Based on this result one can predict, that the chromatin shows also three different levels of opening in that region.

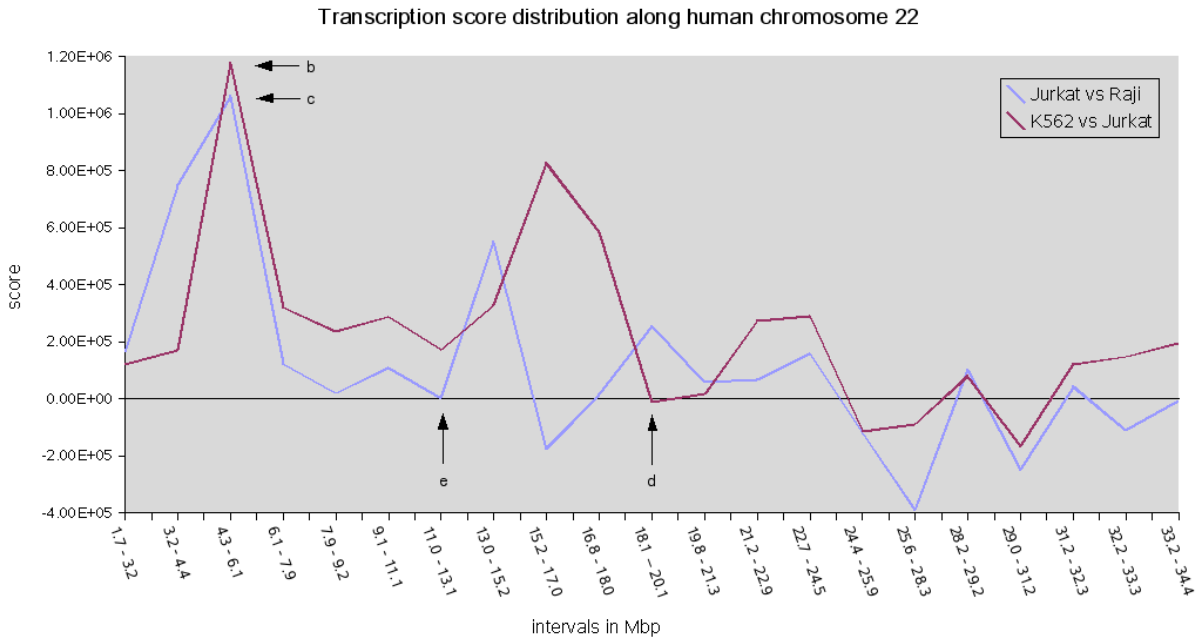


(a) Transcription score distribution

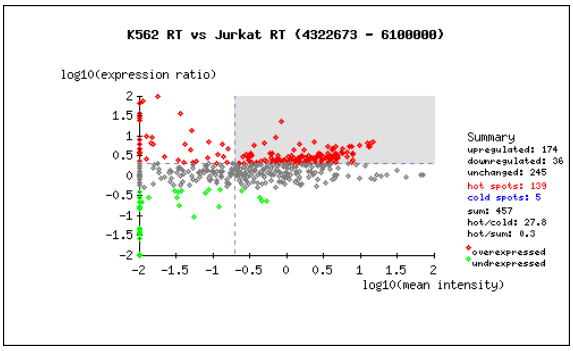


(b) exon expression for b

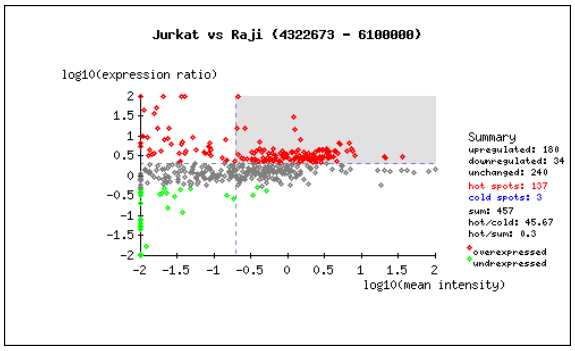


(c) exon expression for c

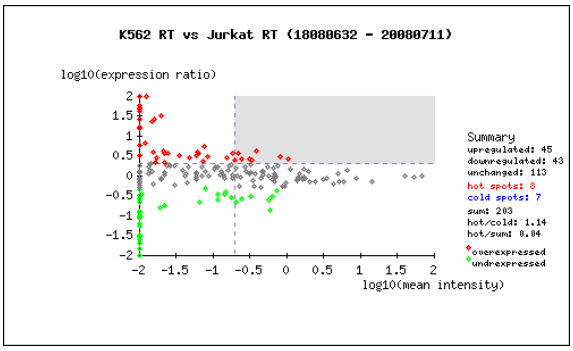


(d) exon expression for d

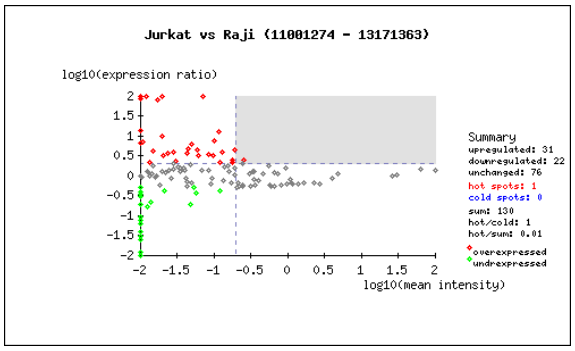


(e) exon expression for e

Figure 4.1: **Transcription plots for "K-562 versus Jurkat" and "Jurkat versus Raji"** for details see 4.1.4 and 4.1.4.1

In figure 4.1a the distribution of the calculated scores along human chromosome 22 for the two comparisons is shown. The arrows b and c mark the score for the region for which a chromatin decondensation, mediated by transcription, is predicted. The score for b means that K-562 is transcriptionally more active compared to Jurkat and thus the chromatin structure should have a more open state. The score c indicates that Jurkat has a higher gene expression than Raji, and thus its chromatin should also be more decondensed.
The arrows e and d indicate regions where the score is nearly 0. Here the transcriptional activity in the two samples is almost identical. In such a region the chromatin structure should not differ between the two compared cell lines.

#### 4.1.4.1 Expression profiles

To visualize the transcriptional activities in the detected regions of potential chromatin decondensation, expression profiles were generated (see 3.1.9). The exon expressions for the indicated regions are shown in figure 4.1. The scatter plots in figure 4.1 (b,c,d,e) display the exon expression profiles in the particular regions. The $\log_{10}$ of the mean intensity of the microarray spots for each exon was plotted versus the $\log_{10}$ of its expression ratio. Overexpressed exons are shown in red, underexpressed in green and exons with no significant change in the expression are shown in gray. An exon was marked as overexpressed when its expression ratio was greater then 2, and as underexpressed when its expression ratio was less then 0.5. The vertical blue dashed line represents the threshold below which errors tend to increase rapidly, because spot intensities are not sufficiently above background intensities. The horizontal blue dashed line displays the threshold above which exons are marked as overexpressed.
Exons in the gray area were named "hot spots". Exons with an expression ratio under 0.5 and a spot intensity over the intensity threshold were named "cold spots". These two classes of exons contributed to the score as follows: "cold spots" scored negatively, "hot spots" positively.
As one can see, the regions b and c, which represent the potential regions of chromatin de-

condensation, have a significant number of "hot spots" compared to the number of "cold spots". In contrast, the regions d and e show almost no difference in the exon expression between the two samples.
The expression profiles helped to validate the scores revealed by the scoring system, because the transcriptional activities are depicted in a very intuitive way.

### 4.1.5 Conclusion

Based on this results one can predict, that the region flanked by BAC 22 and BAC 3, show different levels of chromatin condensation in the three cell lines K-562, Jurkat and Raji. Therefore these cell lines were selected for a study by means of fluorescence in situ hybridization.

## 4.2 Microscopy: FISH

In the second part of this work, the detected region on human chromosome 22 was analyzed in situ using the DNA FISH technique. The bioinformatic analysis predicted that the three cell lines (K-562, Jurkat and Raji) show different chromatin compaction in this region. The DNA FISH approach helped to validate the predictions for the chromatin structure.

### 4.2.1 The probes

The two BACs, that determine start and end of the region, served as probes for the in situ hybridization. The probes were prepared as described in 3.2.1.

#### 4.2.1.1 BAC isolation

Cultures of *E.coli* containing BAC 22 and BAC 3 were started from single colonies and the BACs were isolated with the QIAGEN Large-Construct Kit (QUIAGEN Inc., Valencia, CA, USA). The yield of BAC DNA was $\sim$300 ng/$\mu$l for both. An image of the gel for the determination of DNA quantity is shown in figure 3.5.

#### 4.2.1.2 BAC verification

For a sequence verification, the BACs were end-sequenced and aligned to the sequence of human chromosome 22, using the BLAST tool. Figure 4.2 illustrates the result of the alignment.

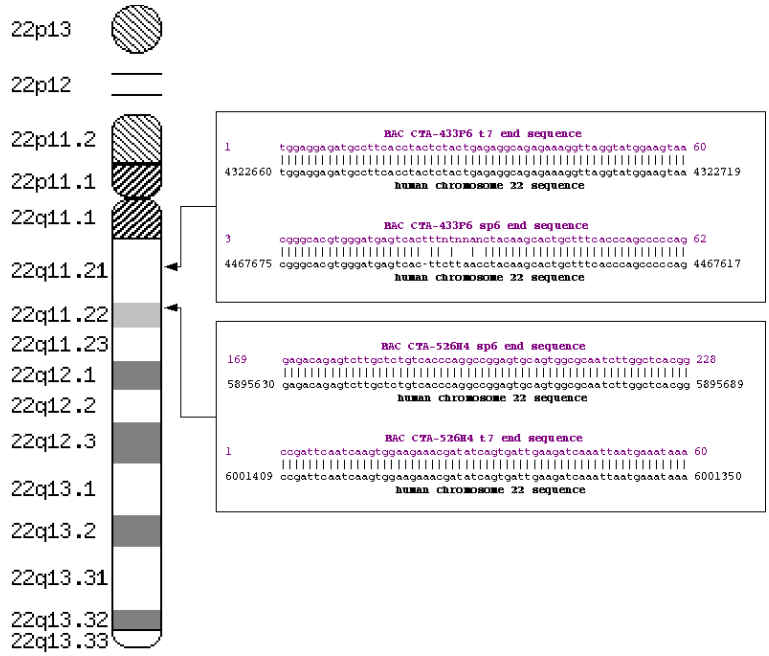


Figure 4.2: **BAC mapping**. Shown is the alignment of the BAC end sequences to chromosome 22. Arrows indicate the position of the matching sequences listed in the boxes.

The alignment shows that the right BACs were isolated. Both of them have a matching sequence on chromosome 22. The t7 end sequence of BAC 22 (CTA-433F6) is located on 22q11.1, 4.3 Mbp downstream from the centromere, which is the start of the region of interest. The t7 end sequence of BAC 3 (CTA-526H4) matches at the end of the region at 22q11.22a, which is 6 Mbp apart form the centromere.

By calculating the distance between the end sequences of a BAC, the sizes of BAC 22 and BAC 3 were determined. The lengths obtained this way were 145 Kbp for BAC 22 and 105 Kbp for BAC 3. With a gel analysis a size of 155 Kbp was determined for BAC 22 and 108 Kbp for BAC 3 respectively (data not shown).

### 4.2.2 Hybridization

The probes were hybridized according to the results of the bioinformatic analysis, as described in 3.2.3, either in pairs or separately to paraformaldehyde fixed cells and detected with avidin-rhodamine. The cells were stained with DAPI and examined with a fluorescence microscope. Images were acquired with a CCD camera and the measurements were done with the MetaMorph Offline program.

#### 4.2.2.1 K-562 and BAC 3

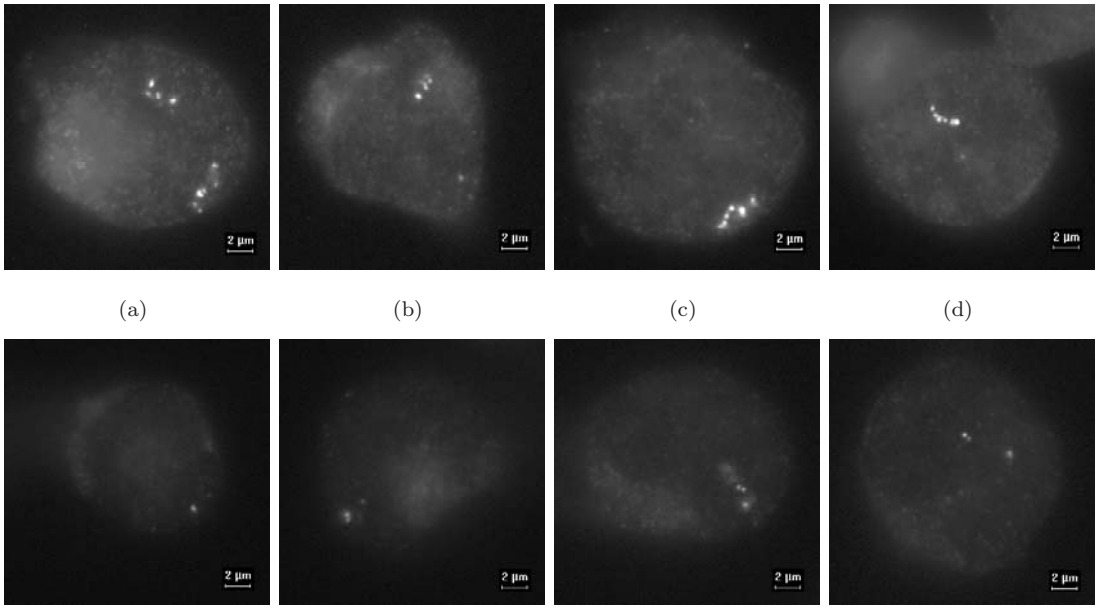


Figure 4.3: **K-562 and BAC 3.** untreated cells: a-d, DRB-treated cells: e-h

In figure 4.3 several images of the hybridization with BAC 3 are shown. The upper panel (a-d) displays untreated K-562 cells, whereas in the lower (e-h) panel the DRB-treated cell are shown. As one can see, the untreated cells have large, open, beady structures, where the BAC hybridizes. In the DRB-treated cells, the BAC can be seen as a dot (e, h) or sometimes as a somewhat bigger structure (f, g). The larger structures can be caused by a incomplete shutdown of transcription. Open structures may also need a long time to

recondense. However, there is a significant difference in the extension of the BAC between treated and untreated cells.

Figure 4.4 shows a histogram where the extension of the BAC in treated and untreated cell is compared. In 40 treated and 41 untreated cells the size of the BAC was measured and the distribution of the measured sizes was plotted. There is a significant shift in the size distribution between the two conditions. The mean size of the BAC in untreated cells is 2.98 $\mu$m compared to 0.7 $\mu$m in treated cells.

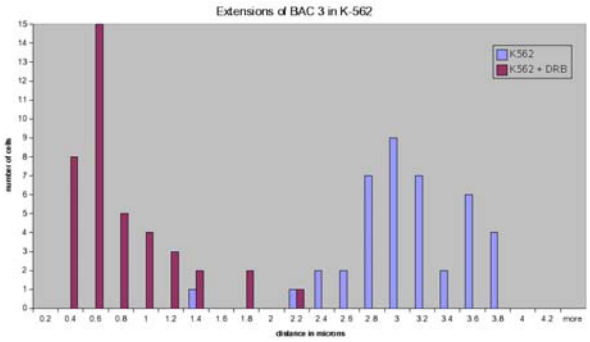


Figure 4.4: **Size distribution**

Due to the large and beady structure of BAC 3 in K-562 it was not possible to distinguish two BACs when BAC 22 was hybridized a the same time together with BAC 3 (data not shown).

To get a better idea of what the structure of BAC 3 looks like, a 3D-Deconvolution was done (by Waltraud Müller). The deconvolved image in figure 4.5 shows a linear structure where beads are connected by fibers . The fibers probably reflect regions of highly decondensed chromatin, whereas the beads represent chromatin in a more condensed state.

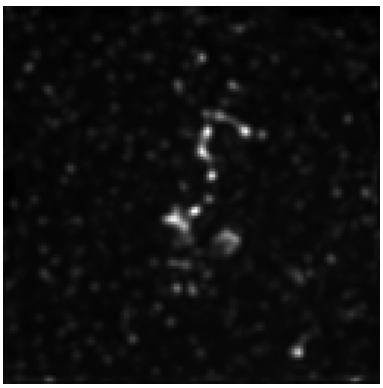

Figure 4.5: **K-562 Deconvolution**

#### 4.2.2.2 K-562 and BAC 3 versus Raji and BAC 3

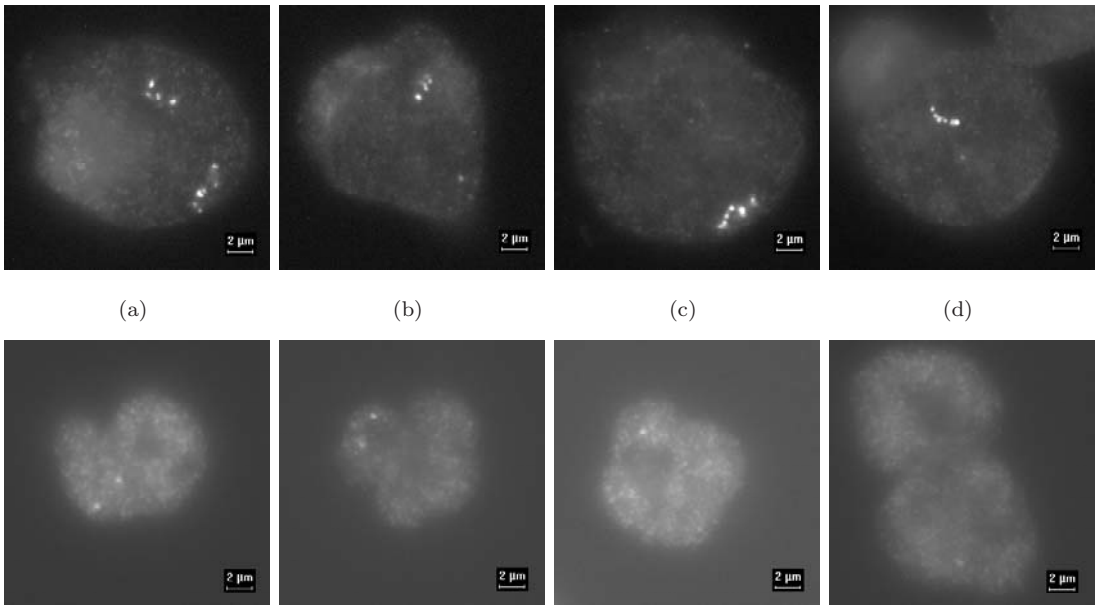


Figure 4.6: **K-562 and BAC 3 (a-d) versus Raji and BAC 3 (e-h)**

Figure 4.6 displays the extension of BAC 3 in two different cell lines. The upper panel (a-d) shows again K-562 cells with the large open structures. As comparison, a hybridization of BAC 3 to Raji cells was done (e-h). In Raji the BAC appears as a dot shaped signal, that means that the chromatin is much more condensed compared to K-562.

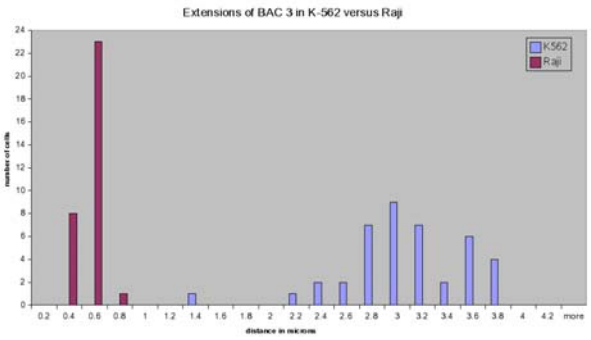


Figure 4.7: **Size distribution**

The histogram 4.7 is a plot of the size distribution in both cell lines. A big shift between the two can be seen. Measurements of BAC 3 in 32 Raji cell revealed a mean length of 0.47 $\mu$m.

#### 4.2.2.3 Amplifications in K-562

The large structures observed, in untreated K-562 cells are hard to explain with a transcription mediated decondensation. The size of BAC 3 is ∼105 Kbp, which corresponds to a linear length of 35.7 $\mu$m. The measurements for the BAC in K-562 revealed a mean length of ∼3 $\mu$m, this corresponds to a DNA compaction rate of 11.9, which seems to be too low compared to the compaction rate of a nucleosome fiber, which is about 6.

A literature search for publications referring to K-562, revealed that there exists an extensive amplification of bcr/abl fusion genes which are clustered on three marker chromosomes [39, 29]. Wu et. al. [39] found that one is large acrocentric, containing 60% of the amplified signals. The second is smaller and contains 30%, while the third contains 10% of the amplified signals. To see if BAC 3 makes part of the amplified region, a metaphase FISH was done. Figure 4.8 shows that the region containing BAC 3 is amplified. It corresponds to the results from Wu et. al. ([39] Fig. 1 B). Rodley et. al. estimated that the amplified components extend proximally from the BCR breakpoint to CRKL [50], resulting in a ∼2.5Mbp amplicon. Estimates of the amplification rate range from 4 to 24 fold. These differences in copy number may signify instability of the amplified fusion gene [50]. An amplification explains the observed structures in K-562. The high score, revealed by the scoring system, is caused by multiple copies of the region. The scoring method was thus able to detect an amplified oncogene, which shows a large-scale chromatin decondensation. This result is consistent with the prediction by Tumbar et. al. who presumed, that naturally occurring gene amplifications, as seen for oncogenes, would tend to give rise to open, extended structures, since they are derived from amplification of active genomic regions [38]. The DRB experiment shows that the region is transcriptional active. This activity results in a decondensation, that recondenses after inhibition with DRB.

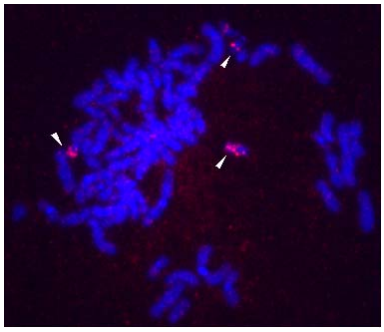

Figure 4.8: **K-562 metaphase FISH**. (by Waltraud Müller) Arrows indicate BAC 3 amplifications.

#### 4.2.2.4 Raji and BAC 3

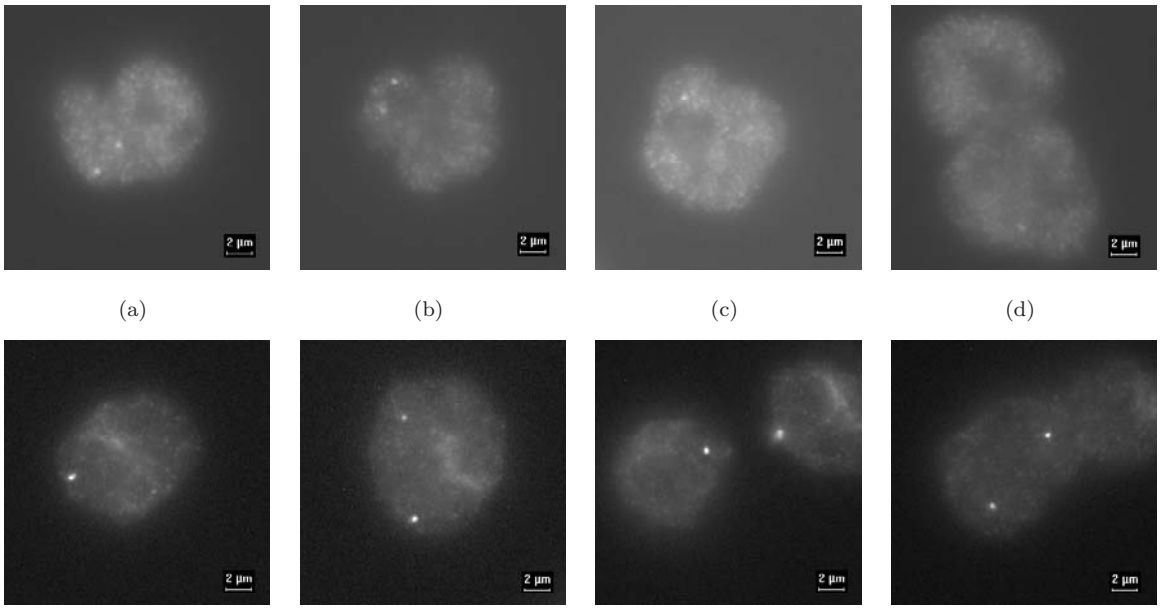


(a) (b) (c) (d)

(e) (f) (g) (h)

Figure 4.9: **Raji and BAC 3** untreated cells: a-d, DRB treated cells e-h

To see if, in Raji cells, the chromatin covered by BAC 3 can be even more condensed the transcription was inhibited by DRB-treatment. The comparison between DRB-treated an untreated Raji cells reveals no significant differences. In figure 4.9 the signal of the BAC is dot shaped in untreated (a-d) and treated (e-h) cells.

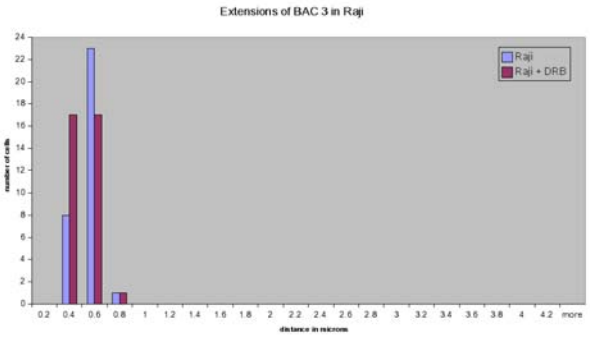


Figure 4.10: **Size distribution**

The measurements of the signals in 35 treated cells resulted in a mean length of 0.43 $\mu$m, which is about the same as in normal cells. Figure 4.10 shows a histogram of the measured sizes for both cases.

#### 4.2.2.5 Jurkat and BAC 3 + BAC 22 versus Raji and BAC 3 + BAC 22

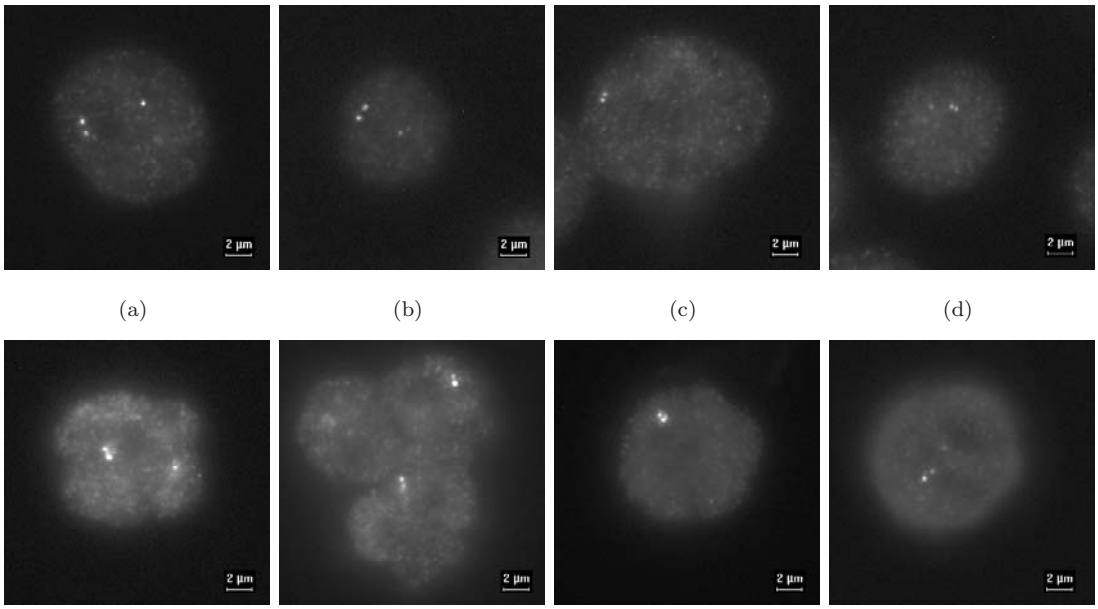


(a) (b) (c) (d)

(e) (f) (g) (h)

Figure 4.11: **Jurkat versus Raji**. Jurkat: a-d, Raji: e-h

The bioinformatic analysis predicted that the chromatin encompassed by BAC 22 and BAC 3 is less condensed in Jurkat cells compared to Raji cells. To test this both BACs were hybridized to Raji and Jurkat cells. The upper panel (a-d) in figure 4.11 displays examples of Jurkat cells, examples of Raji cells are shown below (e-h). In general, the distance between the two BACs in the Jurkat cells (e.g. a and b) is bigger than in the Raji cells (e.g. e, f and g). In a small number of Jurkat cells (e.g. c and d) the distance was comparable to the distance in Raji cells. This can be due to a decreased transcriptional activity in these cases. On the other hand, some Raji cells showed an

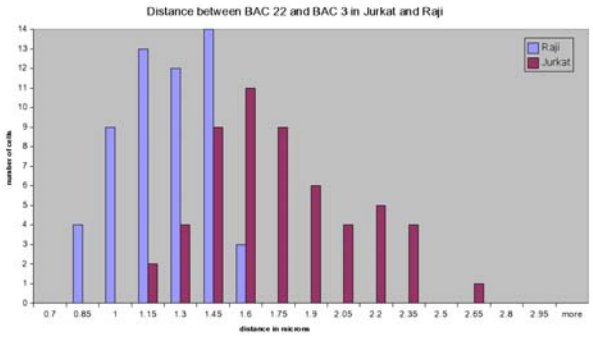


Figure 4.12: **Distance distribution**

increased distance (h).

The histogram in figure 4.12 shows an analysis for multiple cells from both cell lines. From each, the distance in 55 cells was measured and the distribution of the distances was plotted. There is a significant shift from the less active Raji cells to the transcriptionally more active Jurkat cell. As mean distance between the BACs, 1.67 $\mu$m was calculated for Jurkat and 1.18$\mu$m for Raji. However the difference between the biggest distances in both cell lines was more than 1 $\mu$m and the difference between the shortest distance in Raji and the longest in Jurkat was 2.5 $\mu$m.

This result confirms the prediction from the bioinformatic analysis.

#### 4.2.2.6 DRB treated Jurkat and BAC 3 + BAC 22

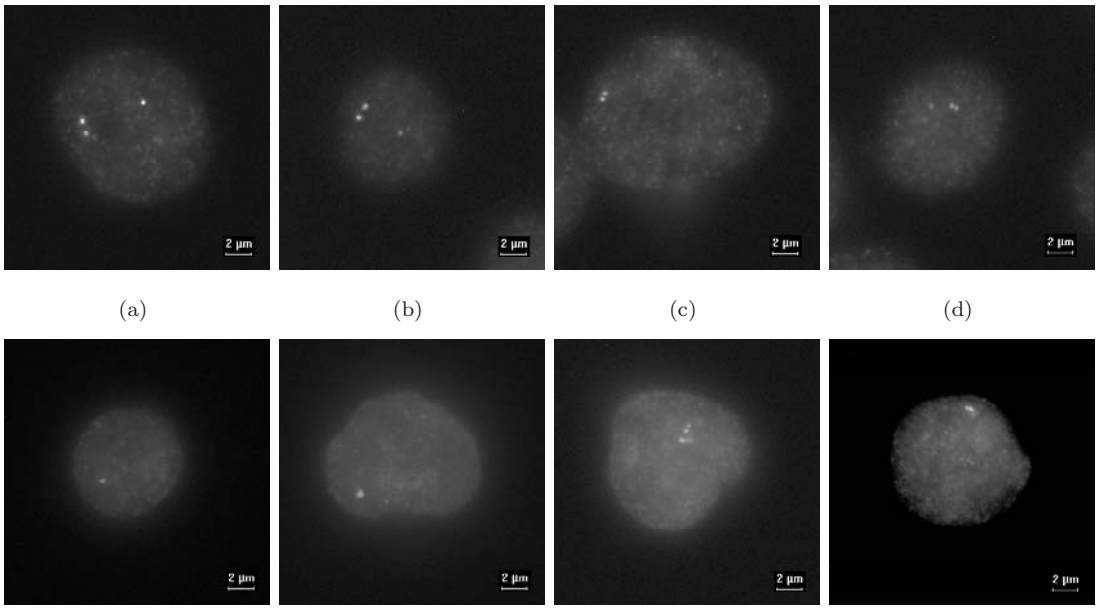


(a) (b) (c) (d)

(e) (f) (g) (h)

Figure 4.13: **Jurkat and BAC 22 + BAC 22**. untreated cells: a-d, DRB treated cells: e-h

To make sure, that the decondensed chromatin structure in Jurkat cells is caused by high transcriptional activity, the two BACs were hybridized to DRB-treated cells. As one can see in figure 4.13, the signals of the two BACs can not always be seen as two separated dots in the treated cells (e and f). In some cases the two signals can be distinguished, but they are still very close (g and h). This can be caused by an incomplete inhibition of transcription through DRB and the long time which is necessary to close open structures. From the comparison with the untreated cells (a-d), one can conclude that there is a transcription triggered chromatin decondensation in the predicted

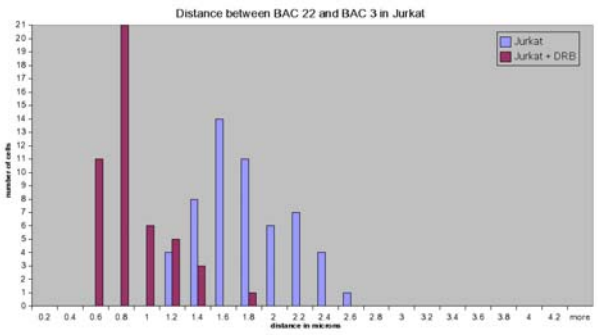


Figure 4.14: **Distance distribution**

region.

The distance distribution plot in figure 4.14 displays nicely the difference in the levels of chromatin opening. The distance between the two BACs in most of the DRB-treated cells is about 0.6-0.8 $\mu$m, whereas the distance of the untreated cells is always bigger than 1 $\mu$m.

### 4.2.3 Chromatin compaction rate

Based on the results of the hybridizations done with two BACs, the chromatin compaction rate for Raji and Jurkat can be estimated. The studied region extends over a distance of ∼1.7 Mbp, which corresponds to a linear distance of 578 $\mu$m. The linear distance is determined by multiplying the number of base pairs by 3.4 Å per nucleotide. The packing ratio is calculated as measured distance divided by linear DNA distance [22].

Table 4.2: Chromatin packing ratio estimations

| **measured extension** | **distance** | **packing ratio** |
|---:|---|---|
| Jurkat max. | 2.57 $\mu$m | 1:225 |
| Jurkat mean | 1.67 $\mu$m | 1:346 |
| Jurkat + DRB min. | 0.41 $\mu$m | 1:1376 |
| Jurkat + DRB mean | 0.78 $\mu$m | 1:741 |
| Raji min. | 0.81 $\mu$m | 1:714 |
| Raji mean | 1.18 $\mu$m | 1:490 |

In table 4.2 the calculated packing ratios are listed. The packing density for the DRB treated Jurkat cells is consistent with the packing ratio of 1,300 found by Müller et. al. [28] for condensed MMTV arrays. The most decondensed Jurkat cells show a ∼5 fold higher condensation than decondensed MMTV arrays, this can be due to a lower transcriptional activity in Jurkat. The comparison of Jurkat versus Raji cells is reflecting the results form the bioinformatic analysis, and shows that the region is less active than in Jurkat.

# Chapter 5

# Discussion

The results of this work suggest that there exist active chromosomal regions which are correlated with large-scale chromatin decondensations.

The bioinformatic analysis of human chromosome 22 microarray data [34], revealed a region that shows different transcriptional activity in three different cell lines, namely K-562, Jurkat and Raji. This region begins 4.3 Mbp apart from the centromere and extends over 1.7 Mbp. In order to find out if this chromosomal region shows transcriptionally mediated changes, such as decondensation, in its large-scale structure, it was investigated by DNA-FISH. Two BAC probes (BAC 22 $\sim$ CTA-433F6, BAC 3 $\sim$ CTA-526G4) flanking the region, were simultaneously hybridized to the interphase chromosomes of the three cell lines. Changes in the large-scale structure were determined by measuring the distances between the fluorescence signals of the two BACs. This approach was chosen, because of the availability of already "FISH-mapped" BACs [52, 10], that were proven to hybridize to unambiguous positions on the chromosome and thus produce clear signals.

In K-562, the cell line that showed the highest transcriptional activity, it was not possible to distinguish two signals, because BAC 3 produced very large linear and beady structures. Thus this single BAC was examined further. Measurements of the extension of the BAC in 40 cells revealed a mean length of $\sim$3 $\mu$m. A metaphase-FISH revealed, that the region in which BAC 3 is located is amplified in K-562. This is consistent with previous studies on this cell line [39, 29, 50], which revealed an extensive amplification of the bcr/abl

oncogene. The long structures, that were observed, can be partially explained by this amplification: The size of BAC 3 is 105 Kbp, that corresponds to a linear length of 35.7 $\mu$m. The measured extension of 3 $\mu$m means a chromatin compaction rate of $\sim$12, which is too low compared to the compaction of the nucleosome fiber and compared to results from previous work [28]. However, to see if also transcription was involved in the formation of the observed structures the cells were treated with DRB, in order to inhibit transcription. The images showed more compact fluorescent signals with a mean extension of $\sim$0.7 $\mu$m, suggesting that a large-scale chromatin decondensation, caused by gene transcription, occurs in the untreated cells. This result is consistent with a prediction by Tumbar et. al., who presumed that large-scale openings in naturally occurring gene amplifications, such as oncogenes, would tend to produce open structures [38].

In Jurkat and Raji it was possible to work with both BACs. The scoring system from the bioinformatic analysis predicted that in Jurkat the distance between the two BACs would be bigger than in Raji. This could be shown by DNA-FISH. The Jurkat cell line was additionally, treated with DRB, in order to examine if the difference in the distances was due to higher transcriptional activity. The treated cells again showed a recondensation of the chromatin in the region, as indicated by the signals which consistently coincided or overlapped.

The results of the FISH experiments lead to the conclusion, that it was possible to predict and identify large-scale chromatin decondensations. Moreover the scoring system which was developed for this work, found a region of an amplified oncogene. The overall results are consistent with the "chromonema fiber" model for higher order chromatin structure, which implies the formation of decondensed fibers over a large range in active chromosomal regions [6, 19]. The deconvolved images of the amplified BAC 3 give an additional clue for the existence of such fibers.

As future aspect, a further investigation of the region with probes covering the entire region would be of interest. The structure in between of the two BACs could then be studied by 3D-deconvolution, which would help to get a better insight in the large-scale chromatin organization.

# Acknowledgments

I want to thank all my supporters, especially my supervisor Zlatko Trajanoski who gave me the great opportunity to conduct the studies for my thesis at the National Institutes of Health.

I want to express my honest gratitude to Waltraud Müller and James McNally who conducted me through the work and from whom I learned a lot: "It was a great honour to work in your group!"

Special thanks go to my girlfriend Lisi for her love, patience and support during my stay in the US.

Finally I want to thank my parents for their support and faith throughout my study.

# Bibliography


[1] Boehringer Mannheim GMBH, Sandhofer Strasse 116, D-68305 Mannheim, Germany. *Biotin-Nick Translation Mix*.

[2] CPAN: Comprehensive Perl Archive Network. WWW. http://www.cpan.org.

[3] Alberts Bruce; Bra Dennis; Lewis Julian; Raff Martin; Roberts Keith; Watson James D.;. *Molecular Biology of the Cell*. Garland Publishing, 3rd edition, 1994.

[4] Stein L. D. GD.pm - Interface to Gd Graphics Library. WWW, 2000. http://search.cpan.org/author/LDS/GD-2.01/GD.pm.

[5] Altschul S.F. et. al. Basic Local Alignment Search Tool. *Journal of Molecular Biology*, 215:403–410, October 1990.

[6] Belmont A. S. et. al. Visualization of G1 Chromosomes: A Folded, Twisted, Supercoiled Chromonema Model of Interphase Chromatin Structure. *The Journal of Cell Biology*, 127:287–302, October 1994.

[7] Belmont A. S. et. al. Large-scale chromatin sturcture and function. *Current Opinion in Cell Biology*, 11:307–311, June 1999.

[8] Bunce T. et. al. DBI - Database independent interface for Perl. WWW, 2002. http://search.cpan.org/author/TIMB/DBI-1.30/DBI.pm.

[9] Caron H. et al. The human transcriptome map: clustering of highly expressed genes in chromosomal domains. *Science*, 291:1289–1292, February 2001.

[10] Cheung V. G. et al. Integration of cytogenetic landmarks into the draft sequqnce of the human genome. *Nature*, 409:953–958, February 2001.

[11] Cho R. J. et al. A genome-wide transcriptional analysis of the mitotic cell cycle. *Mol. Cell*, 2:65–73, July 1998.

[12] Chodosh L.A. et. al. 5,6-dichloro-1-$\beta$-D-ribofuranosylbenzimidazole inhibits transcription elongation by RNA polymerase II in vitro. *Journal of Biological Chemistry*, 264:2250–2257, February 1989.

[13] Cohen B. A. et. al. A computational analysis oh whole-genome expression data reveals chromosomal domains of gene expression. *Nature Gentetics*, 26:183–186, October 2000.

[14] Duggan D. J. et al. Expression profiling using cDNA microarrays. *Nature Genetics*, 21:10–14, January 1999.

[15] Dunham I. et al. The DNA sequence of human chromosome 22. *Nature*, 402:489–495, December 1999.

[16] Dunham I. et al. The DNA sequence of human chromosome 22. WWW, December 1999. http://www.sanger.ac.uk/HGP/Chr22/cwa_archive/Nature_02-12-1999/Chr22Genes.tar.gz.

[17] Dunham I. et al. The DNA sequence of human chromosome 22. WWW, December 1999. http://www.sanger.ac.uk/HGP/Chr22/cwa_archive/Nature_02-12-1999/Chr22Genes.tar.gz.

[18] Hebbes T. R. et al. Core histone hyperacetylation cmaps with generalized DNaseI sensitivity in the chicken $\beta - globin$ chromosomal domain. *EMBO J*, 13:1823–1830, April 1994.

[19] Horn P. J. et. al. Chromatin Higher Order Folding: Wrapping up Transcription. *Science*, 297:1824–1827, September 2002.

[20] Laemmli U. K. et. al. Metaphase Chromosome Structure: The Role of Nonhistone Proteins. *Cold Spring Harb Symp Quant Biol*, 42 Pt 1:351–360, 1978.

[21] Lawrence J. B. et al. Sensitive, High-resolution Chromatin and Chromosome Mapping In Situ: Presence and Orientation of Two Closely Integrated Copies of EBV In a Lymphoma Line. *Cell*, 52:51–61, January 1988.

[22] Lawrence J. B. et al. Interphase and Metaphase Resolution of Different Distances Within the Human Dystrophin Gene. *Science*, 249:928–932, August 1990.

[23] Lichter et al. Analysis of genes and chromosomes by nonisotopic in situ hybridization. *Genetic Analysis, Techniques and Applications*, 8:24–35, February 1991.

[24] Lichter P. et al. Delineation of individual human chromosomes in metaphase and interphase cells by in situ suppression hybridization using recombinant DNA libraries. *Human Genetics*, 80:224–234, November 1988.

[25] Manuelidis L. et. al. A Unified Model of Eukaryotic Chromosomes. *Cytometry*, 11:8–25, 1990.

[26] Marton M. J. et. al. Drug target validation and identification of secondary drug target effects using DNA microarrays. *Nature Medicine*, 4:1293–1301, November 1998.

[27] McNally J. G. et. al. The Glucocorticoid Receptor: Rapid Exchange with Regulatory Sites in Living Cells. *Science*, 287:1262–1265, February 2000.

[28] Müller W. G. et al. Large-scale chromatin decondensation and recondensation regulated by transcription from a natural promoter. *The Journal of Cell Biology*, 154:33–48, July 2001.

[29] Naumann S. et. al. Complete karyotype characterization of the K562 cell line by combined application of G-banding, multiplex-fluorescence in situ hybridization, floures-cence in situ hybridization, and comparative genomic hybridization. *Leukemia Research*, 25:313–322, April 2001.

[30] Orphanides G. et. al. RNA polymerase II elongation through chromatin. *Nature*, 407:471–475, September 2000.

[31] Rigby P.W. et. al. Labeling deoxyribonucleic acid to high specific activity in vitro by nick translation with DNA polymerase I. *Journal of Molecular Biology*, 113:237–251, June 1977.

[32] Roberts C. J. et al. Signaling and Circuitry of Multiple MAPK Pathways Revealed by a Matrix of Global Gene Expression Profiles. *Science*, 287:873–880, February 2000.

[33] Roy P. J. et al. Chromosomal clustering of muscle-expressed genes in Caenorhabditis elegans. *Nature*, 418:975–979, August 2002.

[34] Shoemaker D. D. et al. Experimental Annotation of the Human Genome Using Microarray Technology. *Nature*, 409:922–927, February 2001.

[35] Solovei I. et. al. Spatial Preservation of Nuclear Chromatin Architecture during Three-Dimensional Fluorescence in Situ Hybridization (3D-FISH). *Experimental Cell Research*, 276:10–23, May 2002.

[36] Stadler J. et al. Tissue-specific DNA cleavages in the globin chromatin domain introduced by DNaseI. *Cell*, 20:451–460, June 1980.

[37] Tsukamoto T. et al. Visualization of gene activity in living cells. *Nature Cell Biology*, 2:871–878, December 2000.

[38] Tumbar T. et al. Large-Scale Chromatin Unfolding and Remodeling Induced by VP16 Acidic Activation Domain. *Journal of Cell Biology*, 145:1341–1354, June 1999.

[39] Wu S-Q et. al. Extensive amplification of bcr/abl fusion genes clustered on three marker chromosomes in human leukemic cell line K-562. *Leukemia*, 9:848–862, May 1995.

[40] Albertson D. G. Mapping muscle protein genes by in situ hybridization using biotin labeled probes. *The EMBO Journal*, 4:2493–2498, June 1985.

[41] Albertson D. G. In Situ Hybridization Using Biotin-Labeled Probes. *Trends in Genetics*, 5:3, January 1989.

[42] Rosetta Inpharmatics. Experimental Annotation of the Human Genome Using Microarray Technology. WWW, February 2000. http://download.rii.com/tech/pubs/nature/chromo22.htm.

[43] Rosetta Inpharmatics. Gene Expression Markup Language (GEML). WWW, November 2000. http://www.rosettabio.com/products/conductor/geml/default.htm.

[44] Manuelidis L. Indications of Centromere Movement during Interphase and Differentiation. *Annals of the New York academy of science*, 450:205–221, 1985.

[45] Manuelidis L. Individual interphase chromosome domains revealed by in situ hybridization. *Human Genetics*, 71:288–293, 1985.

[46] Manuelidis L. A View of Interphase Chromosomes. *Science*, 250:1533–1540, December 1990.

[47] Wall L. Perl: Practical Extraction and Report Language. WWW. http://www.perldoc.com/perl5.6/pod/perl.html.

[48] The MySQL AB Company (David Axmark, Allan Larsson and Michael Monty Widenius). The MySQL database management system. WWW. http://www.mysql.com.

[49] Sanford Morton. Chart::Plot - Plot two dimensional data in an image. Version 0.10. WWW, 2000. http://search.cpan.org/author/SMORTON/Chart-Plot-0.11/Plot.pm.

[50] Rodley P. Comparative Genomic Hybridization Reveals Previously Undescribed Amplifications and Deletions in the Chronic Myeloid Leukemia-Derived K-562 Cell Line. *Genes, Chromosomes & Cancer*, 19:36–42, May 1997.

[51] Durbin R. and Haussler D. GFF (General Feature Format) Specifications. WWW, October 1997. http://www.sanger.ac.uk/Software/formats/GFF/GFF_Spec.shtml.

[52] Kirsch I. R. and Ried T. Integration of Cytogenetic Data With Genome Maps and Available Probes: Present Status and Future Promise. *Seminars in Hematology*, 37:420–428, October 2000.

[53] Boutell T. GD Graphics Library. WWW. http://www.boutell.com/gd/.

[54] Hubbard T. GFF Perl Object Modules. WWW, 1999. http://www.sanger.ac.uk/Software/formats/GFF/GFF.shtml.

[55] Razin S. V. The nuclear matrix and chromosomal DNA loops: is their any correlation between partitioning of the genome into loops and functional domains? *Cellular Molecular Biology Letters*, 6:59–69, 2001.

# Index

# Appendix A

# Protocols

## A.1 DNA FISH

### A.1.1 Specimen preparation, hybridization and detection

Use a $\frac{1}{4}$ of a 22x22 mm or a whole 12 mm round coverslip. Harvest cells by a 10 min. centrifugation of 12 ml cell suspension ($70 - 80$ % confluent) and resuspend the pellet in 1 ml of fresh medium. Apply $\sim$60 $\mu$l of the suspension on a 22x22 mm or 30 $\mu$l on a 12 mm round polyslysine-coated coverslip and incubated for one hour at 37°C 5% $CO_2$.

- fix cells by 3.5% PFA for 15 min
- wash 2x5 min. with $PBS^{--}$
- 10 min. permeabilization in 0.5% Triton X 100/ $PBS^{--}$
- wash 3x5 min. with $PBS^{--}$
- treat 20 min. with RNAse 25$\mu$g/ml in $PBS^{--}$ at room temp.
- wash 3x5 min. with $PBS^{--}$
- 10 min. 2xSSC treatment
- wash $\sim$1min. in 70% formamide/2xSSC

- denature at 85°C (Raji + Jurkat 5 min., K562 3.5 min.) in 70% formamide/2xSSC
- dehydrate on ice with 4 min. 70%, 4 min. 90%, 4 min. 100% EtOH
- dry coverslip for 5 min. at room temperature
- add 5$\mu$l probe on a microscope slide and apply the coverslip upside-down
- seal with rubber cement
- hybridize in moist chamber at 37°C over night

**Washes after hybridization:**

- preheat 50% formamide/2xSSC to 45°C and wash the coverslip at room temperature 2x15 min.
- wash 10 min. in 0.1xSSC
- wash 10 min. in 2xSSC

**avidin/rhodamine treatment:**

- prepare a fresh 1:200 avidin/rhodamin in 4xSSC/0.1% BSA/0.01% TWEEN20 solution
- apply $\sim$20$\mu$l of the solution per 1/4 coverslip on a microscope slide.
- place the coverslip upside-down on the slide
- incubate for 45min. at 37°C in moist chamber.

**Washes after avidin/rhodamine treatment:**

- 10 min. 4xSSC/0.1% TWEEN20
- 2x10 min. 4xSSC
- $\sim$10 min. 2xSSC
- coverslips can be stored in PBS$^{--}$ at 4°C.

### A.1.2 Probe preparation

**BAC-DNA at −20°C: ∼300 ng/µl**

- Prepare the following mix:

| |
|---|
| ∼150 ng of BAC DNA = 3 µl nicktranslation (Biotin) |
| 0.7 µl salmon sperm DNA 10 mg/ml |
| 5 µl human cot1 DNA 1 mg/ml |
| 11.3 µl $H_2O$ |
| 1/10 Vol. 3M sodium acetat pH 5.2 |
| 2 Vol. abs. EtOH |
| 20 µl total volume |

**DNA precipitation:**

- put mixture for 30min. on dry ice + EtOH
- spin down at 15000 rpm at room temperature for 15 min.
- rinse 1x with 70% EtOH
- dry for 20 min. at room temperature.

**Hybridization cocktail:**

- add 2.5 µl formamide and 1 µl $H_2O$
- dissolve at 37°C for 20 min. (vortex in between).
- add 0.5 µl 20xSSC and 1 µl 25% dextrane sulfate (mix well before use)

**Denaturation:**

- denature at 85°C for 10 min.

## A.2 Glycerol cultures

- ONC in 2 ml LB 12.5 $\mu$g/ml chloramphenicol, 37°C
- transfer 1.5 ml from each ONC into fresh eppendorf tubes
- spin the cells down for 30 sec.
- discard the supernatant medium
- add 200 $\mu$l LB 12.5 $\mu$g/ml chloramphenicol and resuspend the cell pellet
- add 500 $\mu$l steril glycerol and mix carefully
- store glycerol cultures at $-80$°C

## A.3 Freezing cells for conservation

- collect the cells by centrifugation
- resuspend the pellet in cold freezing medium (=grow medium containing 5-10% DMSO Dimethyl Sulfoxide)
- aliquot cell suspension into labeled freezing vials (Nunc + labeled cap insert)
- cap and place in Nalgene Freezing Container (precooled on ice).
- place loaded freezing container over night in the minus $-80$°C freezer
- place the frozen vials into a liquid nitrogen container

# Appendix B

# Gene-list

Table B.1: Annotated genes in region of interest

| Start bp | End bp | Gene |
|---|---|---|
| 4341617 | 4355088 | zinc finger protein 74 (Cos52) |
| 4371978 | 4379221 | Matches EST sequences |
| 4388912 | 4436631 | Matches EST sequences |
| 4484510 | 4535007 | Homo sapiens mRNA; EST DKFZp586E2117$_r$1 |
| 4576780 | 4577120 | Similar to IGLL sequences |
| 4612030 | 4615254 | Similar to Wp:CE06096, BEM-1/BUD5 SUPPRESSOR-LIKE |
| 4638988 | 4643265 | Similar to Em:AL117401, humam cDNA DKFZp434P211, POM121-like 1 |
| 4642174 | 4643146 | Similar to TR:Q12844 : BREAKPOINT CLUSTER REGION PROTEIN |
| 4647189 | 4648818 | Homo sapiens mRNA; from clone DKFZp434G1017 |
| 4651915 | 4782925 | phosphatidylinositol 4-kinase, catalytic, alpha polypeptide |
| 4723507 | 4731932 | heparin cofactor II |
| 4803249 | 4832187 | synaptosomal-associated protein, 29kD |
| 4861638 | 4894515 | avian sarcoma virus (v-crk) oncogene homolog-like |
| 4918249 | 4925974 | Similar to Tr:O42346, frog TAMEGOLOH |
| 4927322 | 4943982 | leucine-zipper-like transcriptional regulator 1 |
| 4960081 | 4973751 | A novel human P2X receptor gene regulated by p53 |
| 4973640 | 4976773 | Homo sapiens mRNA for cationic amino acid transporter 3 |
| 4987264 | 4989938 | Similar to Sw:O15547, human P2X PURINOCEPTOR 6 (ATP RECEPTOR) |
| 5060849 | 5064675 | BCR like gene |
| 5152896 | 5154638 | gamma-glutamyltransferase 3 |

*continued on next page*

| *continued from previous page* | | |
|---|---|---|
| Start bp | End bp | Gene |
| 5235677 | 5239506 | BCR related |
| 5254896 | 5255442 | Matches EST cluster |
| 5304515 | 5305113 | Similar to Em:X91348, DGCR5 in genomic Em:AC000095 |
| 5333187 | 5334084 | Similar to Tr:O75111, KIAA0612 PROTEIN |
| 5389868 | 5396377 | KIAA1020 protein |
| 5413200 | 5414994 | Matches EST cluster |
| 5417928 | 5433300 | Similar to Em:AF012872, human phosphatidylinositol 4-kinase 230 |
| 5490598 | 5491486 | Similar to Em:AB002316, KIAA0612 |
| 5512636 | 5568940 | ubiquitin-conjugating enzyme E2L3 |
| 5587342 | 5589048 | Similar to Tr:Q99470, Human secretory protein, SDF-2 |
| 5606416 | 5606845 | Matches EST cluster |
| 5610928 | 5641329 | Human cyclophilin-like protein CyP-60 mRNA |
| 5645767 | 5655734 | Homo sapiens unknown mRNA |
| 5705295 | 5707050 | Matches EST cluster |
| 5708005 | 5812536 | protein kinase, mitogen-activated 1 (MAP kinase 1; p40, p41) |
| 5864417 | 5897826 | KIAA0015 |
| 5902021 | 5920802 | Homo sapiens DNA topoisomerase III beta (TOP3b) mRNA |
| 5930513 | 6814186 | Immunoglobulin lambda variable region |
| 5936381 | 5940470 | Similar to Tr:O60813, KIAA0014 LIKE PROTEIN |